Journal of South American Earth Sciences 46 (2013) 9–25

Contents lists available at SciVerse ScienceDirect

Journal of South American Earth Sciences

journal homepage: www.elsevier.com/locate/jsames

Sr–Nd–Pb isotopic constraints on the nature of the mantle sources involved in the genesis of the high-Ti tholeiites from northern Paraná Continental Flood Basalts (Brazil)

Eduardo R.V. Rocha-Júnior [a,b,*], Leila S. Marques [a], Marly Babinski [c], Antônio J.R. Nardy [d], Ana M.G. Figueiredo [e], Fábio B. Machado [f]

[a] Instituto de Astronomia, Geofísica e Ciências Atmosféricas, Universidade de São Paulo, São Paulo, SP 05508-090, Brazil
[b] Instituto de Geociências, Universidade Federal do Rio Grande do Sul, Porto Alegre, RS 91501-970, Brazil
[c] Instituto de Geociências, Universidade de São Paulo, São Paulo, SP 05422-970, Brazil
[d] Instituto de Geociências e Ciências Exatas, Universidade Estadual Paulista, Rio Claro, SP, Brazil
[e] Instituto de Pesquisas Energéticas e Nucleares, Av. Prof. Lineu Prestes 2242, São Paulo, SP 05508-000, Brazil
[f] Departamento de Ciências Exatas e da Terra, Universidade Federal de São Paulo, Diadema, SP, Brazil

ARTICLE INFO

Article history:
Received 8 November 2012
Accepted 20 April 2013

Keywords:
Paraná Continental Flood Basalts
Mantle sources
High-TiO_2 basalts
Sr–Nd–Pb isotopic systematics
Mantle plume

ABSTRACT

There has been little research on geochemistry and isotopic compositions in tholeiites of the Northern region from the Paraná Continental Flood Basalts (PCFB), one of the largest continental provinces of the world. In order to examine the mantle sources involved in the high-Ti (Pitanga and Paranapanema) basalt genesis, we studied Sr, Nd, and Pb isotopic systematics, and major, minor and incompatible trace element abundances. The REE patterns of the investigated samples (Pitanga and Paranapanema magma type) are similar (parallel to) to those of Island Arc Basalts' REE patterns. The high-Ti basalts investigated in this study have initial (133 Ma) $^{87}Sr/^{86}Sr$ ratios of 0.70538–0.70642, $^{143}Nd/^{144}Nd$ of 0.51233–0.51218, $^{206}Pb/^{204}Pb$ of 17.74–18.25, $^{207}Pb/^{204}Pb$ of 15.51–15.57, and $^{208}Pb/^{204}Pb$ of 38.18–38.45. These isotopic compositions do not display any correlation with Nb/Th, Nb/La or P_2O_5/K_2O ratios, which also reflect that these rocks were not significantly affected by low-pressure crustal contamination. The incompatible trace element ratios and Sr–Nd–Pb isotopic compositions of the PCFB tholeiites are different to those found in Tristan da Cunha ocean island rocks, showing that this plume did not play a substantial role in the PCFB genesis. This interpretation is corroborated by previously published osmium isotopic data (initial γ_{Os} values range from +1.0 to +2.0 for high-Ti basalts), which also preclude basalt generation by melting of ancient subcontinental lithospheric mantle. The geochemical composition of the northern PCFB may be explained through the involvement of fluids and/or small volume melts related to metasomatic processes. In this context, we propose that the source of these magmas is a mixture of sublithospheric peridotite veined and/or interlayered with mafic components (e.g., pyroxenites or eclogites). The sublithospheric mantle (dominating the osmium isotopic compositions) was very probably enriched by fluids and/or magmas related to the Neoproterozoic subduction processes. This sublithospheric mantle region may have been frozen and coupled to the base of the Parana basin lithospheric plate above which the Paleozoic subsidence and subsequent Early Cretaceous magmatism occurred.

1. Introduction

Continental Flood Basalts (CFB) represent major, short-lived igneous events on Earth, and are responsible for the addition of new juvenile material to the continental crust (White and McKenzie, 1989). Recent studies about large CFB, as well as about associated geodynamic processes, has been widely investigated and discussed in the literature. However, their genesis remains a very controversial subject (e.g., Sheth, 2005; Anderson, 2005). Although some CFB are related to mantle plume activity, other CFB may be more directly linked to heterogeneous sources present either in the lithospheric mantle (Bellieni et al., 1984; Hawkesworth et al., 1992) or in the shallow mantle (e.g., Meibom and Anderson, 2003). Many CFB have compositions that differ substantially from those of oceanic basalts

* Corresponding author. Present address: Instituto de Geociências, Universidade Federal do Rio Grande do Sul, Porto Alegre, RS 91501-970, Brazil. Tel.: +55 51 3308 7287.
E-mail addresses: eduardofisica@yahoo.com.br, eduardofisica@gmail.com (E.R.V. Rocha-Júnior).

0895-9811/$ – see front matter © 2013 Elsevier Ltd. All rights reserved.
http://dx.doi.org/10.1016/j.jsames.2013.04.004

and these variations have been attributed to differences in their mantle source regions and/or to crustal contamination.

According to Lustrino (2005), the geographic locations of CFB are not random but invariably associated with ancient mobile belts. This may be considered as evidence for strong structural control of both the crustal and mantle portions of the lithosphere in channelling the CFB feeding systems.

The Paraná continental flood basalt (PCFB) province, one of the largest CFB provinces, has been the subject of many studies and there has been much controversy about the processes involved in the basalt genesis. Gibson et al. (1995, 1999, 2005) and Ewart et al. (1998) suggested that the flood basalt compositions substantially reflect a deep asthenospheric mantle plume (Tristan da Cunha) source. The plume model invokes vertical introduction of thermally anomalous source material for intraplate volcanism. Peate et al. (1999) and Marques et al. (1999) proposed that the flood basalts were originated by heterogeneous lithospheric mantle melting and this plume could have acted as a heat source for this process. In addition, Ernesto et al. (2002) proposed an alternative non-plume-related model for the generation of PCFB by using geochemical, isotope, paleomagnetic and geoid anomaly data. According to those authors the magmatism was triggered by a large thermal anomaly, located at the coast of Western Africa, over which Paraná Basin remained almost stationary for about 50 Ma. It is also worth noting that the PCFB was closely associated with the opening of the South Atlantic Ocean during Early Cretaceous (Piccirillo and Melfi, 1988; Hawkesworth et al., 1992).

In this context, the possible influence of an ancient subcontinental lithospheric mantle (SCLM), Tristan da Cunha plume (OIB – ocean island basalt) or an asthenospheric mantle source (depleted mantle) on the formation of the PCFB was investigated by Rocha-Júnior et al. (2012) based on new Re–Os isotopic data, which showed that exclusive melting of either ancient SCLM or mantle-plume (Tristan da Cunha) cannot satisfactorily explain the overall chemical and isotopic features of the PCFB. According to these authors, the asthenospheric component involved in the generation of the PCFB, was enriched by fluids and/or magmas related to the Neoproterozoic subduction processes, and this sub-lithospheric mantle region may have been frozen and coupled to the base of the Paranapanema Craton.

The main objectives of the present study include: (1) geochemical and isotope (Sr, Nd, and Pb) studies of tholeiitic rocks, which outcrop in Northern region of PCFB in order to obtain additional constraints about their genesis; (2) evaluation of contributions from different sources to the petrogenesis of the rocks; (3) improve the relatively poorly known Pitanga and Paranapanema magma-types of the PCFB in isotopic terms. The peculiarity of these rocks in terms of both trace elements and Sr–Nd–Pb isotopic ratios is pointed out, and a model to constrain the mantle sources of this volcanism is attempted.

2. Geological setting

Basalts of the PCFB province are of Early Cretaceous age and were emplaced on a large intracratonic Paleozoic sedimentary basin (Paraná Basin) that started subsiding in the Early Paleozoic. This basin is located in terrains of the South American platform which were extensively affected by the tectonic, metamorphic and magmatic events of the Brasiliano/Pan-African orogenic cycle, whose most important accretion episodes are the ones between 650 and 500 Ma (e.g., Cordani et al., 2003). The geological character, age and composition of the oldest basement rocks below the Paraná Basin are mostly unknown.

The PCFB covers an area of about 1,200,000 km^2 and comprises 780,000 km^3 of extrusive material (Piccirillo and Melfi, 1988). Associated to the volcanic activity there was intrusive magmatism, represented by sills, which outcrop mainly in the Eastern and Northeastern Paraná Basin, and dyke swarms (Ponta Grossa, Serra do Mar, and Florianópolis; Piccirillo et al., 1990; Raposo et al., 1998; Deckart et al., 1998).

Geochronological data (based on $^{40}Ar/^{39}Ar$ method) show that the main volcanic activity in the PCFB occurred within a short time interval between 133 and 132 Ma (Renne et al., 1992; Turner et al., 1994), before of the South America and Africa separation. Most recently, Thiede and Vasconcelos (2010) placed PCFB extrusion at 134.6 ± 0.6 Ma (consistent with previous data, considering the new defined K decay constants), concluding that the duration of the PCFB volcanism was <1.2 Ma. In addition, Janasi et al. (2011) reported the first U–Pb baddeleyite/zircon dates on felsic volcanic rocks from the PCFB, with an age of 134.3 ± 0.8 Ma, confirming the idea that this magmatic event were emplaced over a very short period of ~1 Ma.

Previous geological and geochemical studies (e.g., Bellieni et al., 1984; Piccirillo and Melfi, 1988; Peate et al., 1992; Marques et al., 1999) allowed the division of PCFB into two main regions: (1) Southern PCFB is characterized by the occurrence of tholeiitic basalts with dominantly low-Ti (LTi; $TiO_2 \leq 2$ wt.%) and low concentrations of incompatible elements, such as P, Ba, Sr, Zr, Hf, Ta, Y, and light rare earth elements (LREE); (2) the Northern PCFB is characterized by tholeiites with mostly high concentrations of TiO_2 (HTi; $TiO_2 > 2$ wt.%) and incompatible elements.

Based on titanium and incompatible trace elements (Sr, Y, and Zr), which are generally immobile during hydrothermal alteration and weathering processes, Peate et al. (1992) divided the basaltic rocks from PCFB in six magma-types. The HTi basalts were divided in three groups: Urubici (HTi-Southern: $TiO_2 > 3$ wt.%; Sr > 550 μg/g; Ti/Y > 500), Pitanga (ATi-Northern: $TiO_2 > 3$ wt.%; Sr > 350 μg/g; Ti/Y > 350), and Paranapanema (ITi-Northern: $2 < TiO_2 < 3$ wt.%; 200 < Sr < 450 μg/g; Ti/Y > 330). The LTi basalts were also divided in three ones: Gramado (BTi-Southern: $TiO_2 < 2$ wt.%; 140 < Sr < 400 μg/g; Ti/Y < 300), Esmeralda (LTi-Southern: $TiO_2 < 2$ wt.%; 120 < Sr < 250 μg/g; Ti/Y < 330), and Ribeira (LTi-Northern: $TiO_2 < 2$ wt.%; 200 < Sr < 375 μg/g; Ti/Y > 300). In the area which is investigated in the present study, Pitanga and Paranapanema magma-types are usually found.

With respect to sampling, the studied rocks were sampled in the northern part of the PCFB province (Fig. 1). All samples belonging to Pitanga and Paranapanema magma-types are lava flows, except one sample for Pitanga (KS-649), and two for Paranapanema (KS-660 and KS-671), which are sills. Sample locations are shown in Fig. 1.

3. Analytical techniques

Fifty-seven samples (47 belonging to Pitanga and 10 samples belonging to Paranapanema) were selected for major, minor and some trace elements (Cr, Ni, Sr, Y, Zr and Nb) by X-ray florescence, at the Instituto de Geociências e Ciências Exatas, Universidade Estadual Paulista (UNESP, Brazil). In these samples, the concentrations of rare earth elements and other incompatible trace elements (e.g., Ta, Th, U, and Hf) were also determined by instrumental neutron activation analysis at the Instituto de Pesquisas Energéticas e Nucleares (IPEN/SP, Brazil). Precision and accuracy are better than 5% for major and minor elements, and better than 10% for trace elements (Nardy et al., 1997; Rocha-Júnior, 2011).

Twenty out of these samples were selected for Sr, Nd, and Pb isotope analysis. Isotopic measurements were carried out at the *Centro de Pesquisas Geocronológicas*, Instituto de Geociências, Universidade de São Paulo (USP, Brazil) by thermal ionization mass-spectrometry (TIMS). Sr and Nd isotopic compositions were determined according to the analytical procedures described by

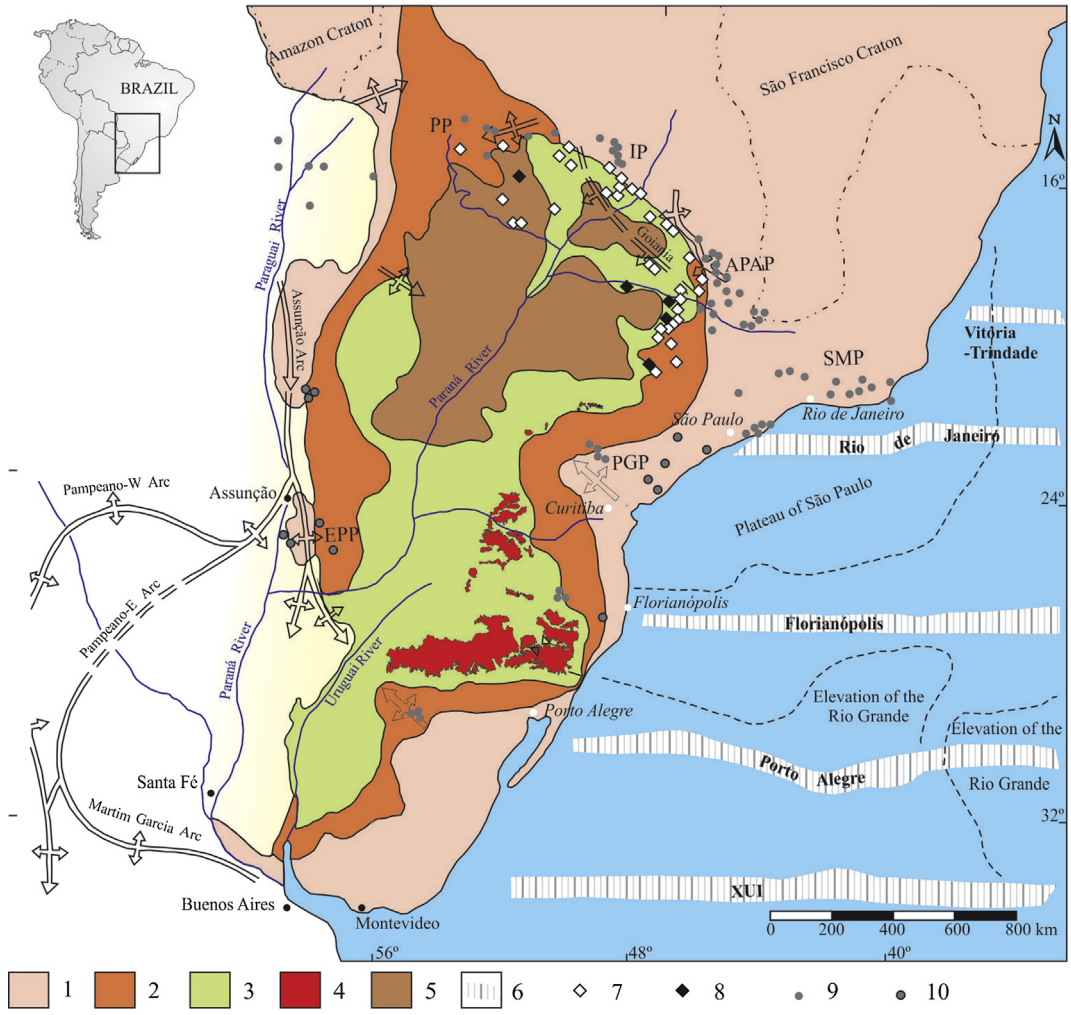

Fig. 1. Generalized geological map of the studied area. (1) Crystalline basement; (2) pre-volcanic sediments (mainly Paleozoic); (3) basic to intermediate flood volcanics (PCFB); (4) acid lava flows of Chapecó and Palmas types (PCFB); (5) post-volcanic sediments (mainly Late Cretaceous); (6) oceanic lineament; (7) Pitanga samples analyzed in this study; (8) Paranapanema samples analyzed in this study; (9) and (10) correspond to the location of the alkaline and alkaline–carbonatitic complexes in and around the PCFB. Data sources: Piccirillo and Melfi (1988), Gibson et al. (1997), Marques et al. (1999), Carlson et al. (2007).

Kawashita (1972) and Sato et al. (1995), using a Finnigan MAT 262 mass spectrometry. The Sr isotopic ratios were normalized to $^{86}Sr/^{88}Sr = 0.1194$ and replicate analyses of $^{87}Sr/^{86}Sr$ for the NBS987 standard gave a mean value of 0.71028 ± 0.00006 (2σ); analytical blanks were less than 0.3 ng. The Nd isotopic compositions were normalized to $^{146}Nd/^{144}Nd = 0.72190$. The averages of $^{143}Nd/^{144}Nd$ for La Jolla and BCR-1 standards were 0.511847 ± 0.00005 (2σ) and 0.512662 ± 0.00005 (2σ), respectively; during this work, the blanks were less than 0.1 ng.

The chemical procedures for the Pb isotope determinations have been given by Babinski et al. (1999) and Marques et al. (1999). The mass fractionation correction was 0.11%/a.m.u., 0.11%/a.m.u. and 0.07%/a.m.u. for $^{206}Pb/^{204}Pb$, $^{207}Pb/^{204}Pb$ and $^{208}Pb/^{204}Pb$, respectively; blanks recorded during the analyses were lower than 100 pg, which are negligible compared to the quantities of Pb separated from the PCFB rocks, typically less than 0.2%.

4. Results

4.1. Major and trace elements

The PCFB, mainly its southern region, have been the subject of previous detailed chemical and mineralogical studies (e.g., Bellieni et al., 1984; Piccirillo and Melfi, 1988; Peate et al., 1992; Marques et al., 1999). The northern part of the PCFB is still lacking in detailed geochemical studies, thus, additional major and trace element data for basalts in the northern PCFB are given in Tables 1 and 2. To make the data set internally consistent, the major and minor elements are normalized to 100% on a volatile-free basis.

The investigated rocks are all basalts or basaltic andesites in composition with SiO_2 ranging from 49 to 53 wt.% according to the TAS classification (Le Bas and Streckeisen, 1991, Fig. 2). Magnesium contents range from 3.7 to 5.6 wt.%. Compositionally, all samples investigated are tholeiitic basalts, presenting high Fe/Mg ratios ($Fe_2O_{3T}/MgO \sim 2.6–4.3$) with relatively high silica contents (wt.% $SiO_2 = 49–53$; Table 1 and Fig. 3).

All of the analyzed samples have TiO_2 contents of 2.6–4.4 wt.% and Ti/Y ratios of 376–736 and belong to the high-Ti basalt group (Marques et al., 1999; Peate et al., 1992; Piccirillo and Melfi, 1988). Of this high-Ti group we can distinguish two magma-types, which emerge from the major and trace element compositions, and they are referred as Pitanga (predominant) and Paranapanema (subordinate), according to the parameters proposed by Peate et al. (1992).

Major elements show strong correlation with MgO (Fig. 3). In general, both Pitanga and Paranapanema rocks display at decreasing MgO, increasing SiO_2, TiO_2, Na_2O, P_2O_5 and K_2O, and

Table 1
Major element data for Pitanga and Paranapanema rocks from northern PCFB.

Sample	SiO_2	TiO_2	Al_2O_3	Fe_2O_3	MnO	MgO	CaO	Na_2O	K_2O	P_2O_5	LOI	Total
Pitanga rocks												
KS-616	48.40	4.36	12.25	16.24	0.22	4.57	8.88	2.24	1.23	0.38	0.66	99.44
KS-620	51.35	3.25	12.67	14.83	0.23	3.64	7.05	2.92	2.15	0.78	0.22	99.91
KS-622	50.96	3.44	12.78	14.88	0.23	4.01	7.94	2.58	1.70	0.42	0.38	99.73
KS-623	50.40	3.44	12.92	14.92	0.21	3.88	8.10	2.59	1.67	0.43	0.38	99.50
KS-625	51.60	3.89	12.59	15.74	0.22	3.78	7.99	2.62	1.39	0.61	0.34	99.57
KS-626	50.83	3.36	12.93	14.93	0.20	3.88	7.75	2.52	1.78	0.44	0.38	99.77
KS-627	50.04	3.63	12.95	14.76	0.22	4.10	8.00	2.57	1.55	0.46	0.66	99.75
KS-628	51.03	3.84	12.49	15.72	0.21	3.68	7.92	2.63	1.51	0.62	0.47	99.15
KS-630	50.30	3.62	12.96	15.01	0.20	3.87	8.00	2.60	1.59	0.49	0.33	99.71
KS-632	50.98	3.86	12.58	15.74	0.21	3.72	7.93	2.78	1.39	0.62	0.60	99.74
KS-633	50.10	3.59	12.74	14.91	0.22	4.53	8.32	2.48	1.62	0.48	0.68	100.55
KS-638	50.42	3.49	13.11	14.75	0.20	4.76	8.96	2.34	1.39	0.41	0.23	99.74
KS-649	49.25	3.97	12.25	15.64	0.22	4.14	8.23	2.46	1.59	0.45	0.65	100.01
KS-658	50.47	3.87	12.80	15.90	0.23	4.48	8.68	2.49	1.37	0.55	0.17	99.78
KS-681	50.52	3.60	13.05	14.81	0.20	3.96	8.15	2.64	0.91	0.49	1.76	100.04
KS-682	50.60	3.85	12.45	15.68	0.21	3.81	7.77	2.52	1.74	0.62	0.85	100.02
KS-683	49.39	3.86	12.58	14.85	0.22	3.94	7.84	2.51	1.89	0.63	1.01	99.93
KS-684	49.39	3.58	13.19	14.40	0.22	4.81	9.20	2.32	0.86	0.42	1.33	99.72
KS-695	49.89	3.51	13.08	14.68	0.20	4.79	9.11	2.27	1.16	0.42	1.13	100.24
KS-696	49.22	3.49	12.98	14.53	0.18	5.17	9.14	2.17	1.00	0.41	1.99	100.28
KS-697	49.61	3.48	13.08	14.68	0.20	4.96	9.16	2.33	1.03	0.41	1.07	100.01
KS-698	49.68	3.50	13.03	14.62	0.20	4.86	9.16	2.26	1.06	0.40	1.16	99.93
KS-700	49.85	3.51	13.10	14.64	0.20	4.90	9.19	2.35	0.94	0.41	1.50	100.59
KS-701	50.14	3.52	13.19	14.77	0.19	4.81	9.17	2.42	0.99	0.41	0.83	100.44
KS-702	49.91	3.50	13.14	14.69	0.21	4.78	9.19	2.49	0.88	0.41	1.01	100.21
KS-746	49.15	3.13	12.80	16.00	0.21	4.07	8.62	2.35	1.29	0.43	1.03	99.08
KS-747	49.17	3.51	12.77	15.84	0.22	4.14	8.41	2.43	1.35	0.47	0.94	99.25
KS-749	48.69	3.29	13.50	14.44	0.18	5.57	9.58	2.36	0.98	0.27	1.22	100.08
KS-756	50.77	3.33	13.21	15.36	0.20	4.57	8.29	2.50	1.48	0.43	0.81	100.95
KS-759	49.63	3.78	13.07	15.12	0.21	4.74	9.11	2.75	0.70	0.45	1.20	100.76
KS-760	50.10	3.70	13.07	15.34	0.21	4.52	8.64	2.60	1.10	0.50	1.17	100.95
KS-762	52.56	3.57	13.31	13.28	0.20	4.12	7.94	2.95	1.38	0.52	1.06	100.89
KS-763	50.30	3.81	12.75	15.52	0.22	3.89	8.01	2.85	1.23	0.62	1.80	101.00
KS-764	48.92	3.23	13.55	14.41	0.20	5.36	9.87	2.48	0.65	0.36	1.42	100.45
KS-765	49.18	3.21	13.43	14.41	0.19	5.28	9.88	2.36	0.76	0.36	1.83	100.89
KS-770	50.72	3.53	13.31	14.30	0.20	3.99	7.91	2.50	1.94	0.53	1.95	100.88
KS-772	50.06	3.74	13.48	13.91	0.20	4.28	8.35	2.94	1.04	0.52	1.58	100.10
KS-775	53.16	3.08	12.83	14.28	0.22	3.74	7.45	2.93	1.90	0.63	0.71	100.93
KS-778	49.70	3.75	12.70	16.20	0.23	4.44	8.49	2.48	1.45	0.53	0.95	100.92
KS-786	50.08	3.58	13.26	13.93	0.21	4.90	9.21	2.48	1.00	0.42	0.99	100.06
KS-787	50.13	3.58	13.27	13.96	0.21	4.98	9.31	2.45	0.99	0.42	0.79	100.09
KS-788	49.96	3.54	13.22	14.03	0.21	4.85	9.22	2.62	0.85	0.43	1.09	100.02
KS-790	50.77	3.90	12.58	15.06	0.22	3.99	8.18	2.68	1.32	0.62	0.86	100.18
KS-793	49.27	3.28	13.62	14.43	0.19	4.74	9.96	2.28	0.69	0.35	1.16	99.97
KS-794	49.05	3.74	13.07	15.57	0.21	4.46	8.70	2.91	0.81	0.48	1.02	100.02
KS-810	49.32	3.62	13.32	15.60	0.20	4.34	8.74	2.33	1.34	0.42	0.62	99.85
LM-2	49.78	3.52	13.25	13.54	0.19	4.34	8.51	2.72	1.01	0.42	1.71	99.01
Paranapanema rocks												
KS-624	49.26	2.98	13.03	15.78	0.22	5.46	9.40	2.56	0.88	0.28	0.14	99.99
KS-660	50.11	2.60	13.33	14.93	0.20	5.48	9.35	2.25	1.07	0.24	0.42	99.98
KS-671	49.90	2.70	13.25	15.16	0.21	5.38	9.62	2.21	1.06	0.35	0.26	100.10
KS-685	49.70	2.84	12.59	15.29	0.28	4.87	9.20	2.30	0.66	0.29	2.09	100.11
KS-703	50.31	2.62	12.96	15.5	0.22	4.65	9.18	2.48	0.83	0.38	1.44	100.57
KS-704	50.31	2.61	13.04	15.36	0.23	4.68	9.33	2.5	0.68	0.37	1.28	100.39
KS-705	50.33	2.63	13.09	15.36	0.22	4.73	9.38	2.51	0.67	0.37	1.1	100.39
KS-706	48.74	2.56	13.05	15.6	0.26	5.26	9.56	2.32	0.76	0.37	1.91	100.39
KS-707	50.25	2.63	13.07	15.3	0.22	4.58	9.18	2.47	0.8	0.38	1.2	100.08
KS-755	51.04	2.87	13.19	15.13	0.2	4.77	8.96	2.45	1.23	0.3	0.78	100.92

All abundances expressed in wt.%. LOI, loss on ignition.

decreasing CaO and Al_2O_3 (Fig. 3). Although some scatter is observed, the trends are compatible with fractional crystallization, and form a continuous, evolutionary trend, which is consistent with literature data (Bellieni et al., 1984; Piccirillo and Melfi, 1988; Peate et al., 1992).

The Paranapanema rocks have MgO contents higher than ~4.6 wt.% (4.6–5.5 wt.%), whereas Pitanga rocks vary from 3.6 to 5.6 wt.%. At similar MgO contents, Paranapanema rocks contain higher SiO_2, Fe_2O_3(t) and lower P_2O_5 than Pitanga. Besides the slightly lower concentrations of TiO_2 ($TiO_2 < 3.0$ wt.%; Fig. 3), Paranapanema rocks are characterized by the lowest abundances of large ion lithophile elements (LILE) and LREE, as well as the lower concentrations of high field strength elements (HFSE) than the Pitanga rocks ($TiO_2 \geq 3.0$ wt.%; Fig. 4).

The investigated rocks show positive correlations between compatible trace elements (i.e., Ni, Sc, Cr, Co; Fig. 5) and MgO, although the most evolved samples have variable Ni contents. Incompatible elements such as Nb, Th, U, Ta, and La generally increase with the degree of differentiation (MgO [not shown], Zr; Fig. 4). This provides strong evidence in favour of their genetic

Table 2
Trace element data for Pitanga and Paranapanema rocks from northern PCFB.

Sample	Ni	Co	Cr	Sc	Sr	Rb	Ba	Zr
Pitanga rocks								
KS-616	28.0	37.3	105	35.5	561	24.1	355	239
KS-620	27.0	33.8	74	24.3	519	40.8	617	334
KS-622	24.5	40.8	67	32.4	455	38.6	527	272
KS-623	25.6	40.7	58	32.2	468	31.8	461	270
KS-625	28.8	38.8	109	32.6	460	31.9	515	309
KS-626	23.6	37.2	78	25.8	455	35.7	525	291
KS-627	24.7	43.2	136	34.6	449	35.5	496	266
KS-628	22.3	36.7	131	31.0	461	33.2	524	302
KS-630	21.2	38.7	80	32.4	449	31.8	444	268
KS-632	21.4	39.2	113	29.8	462	35.1	570	307
KS-633	29.3	37.1	66	28.9	447	32.4	444	278
KS-638	50.8	37.8	109	34.4	438	38.4	432	232
KS-649	64.3	40.0	135	31.0	426	33.0	413	234
KS-658	19.8	41.6	101	33.3	440	24.6	359	212
KS-681	24.7	41.0	85	32.0	510	35.0	374	307
KS-682	21.6	38.3	56	30.8	496	41.3	523	326
KS-683	17.6	38.0	41	30.0	505	36.0	520	340
KS-684	96.4	49.9	120	32.7	472	20.5	450	257
KS-695	53.5	40.4	140	32.0	580	13.1	475	241
KS-696	57.3	37.0	108	31.3	478	14.0	477	240
KS-697	59.1	38.0	121	31.2	566	24.2	397	237
KS-698	56.8	37.5	141	29.7	601	25.7	376	242
KS-700	50.6	42.2	97	36.5	474	22.9	422	234
KS-701	54.5	21.9	106	36.8	467	12.3	393	237
KS-702	54.8	37.1	117	28.9	474	21.4	429	242
KS-746	37.6	41.2	110	37.2	344	30.3	406	196
KS-747	55.7	46.1	132	34.2	364	22.9	475	164
KS-749	58.0	41.9	84	24.3	444	22.3	282	168
KS-756	54.0	44.5	95	32.2	495	35.9	483	246
KS-759	36.0	42.0	126	35.9	421	27.1	383	226
KS-760	45.0	45.1	118	34.8	405	27.5	447	201
KS-762	32.0	35.3	113	29.0	451	36.4	593	283
KS-763	21.0	39.6	89	33.7	455	32.4	514	261
KS-764	75.0	44.9	190	34.6	415	20.0	343	210
KS-765	73.0	46.3	174	35.9	436	17.2	402	208
KS-770	43.0	38.0	63	27.6	437	50.3	519	247
KS-772	31.0	33.7	94	27.8	444	33.3	498	232
KS-775	24.0	29.6	84	27.8	438	41.8	603	283
KS-778	27.0	44.9	63	38.6	362	32.6	447	220
KS-786	68.0	44.2	163	34.8	526	19.6	470	231
KS-787	59.0	42.8	135	34.8	476	21.7	395	228
KS-788	22.0	39.3	160	31.1	547	27.0	442	262
KS-790	66.0	44.8	153	35.5	475	23.1	398	226
KS-793	86.0	47.5	190	35.3	489	17.5	352	207
KS-794	40.0	44.0	165	33.4	500	23.6	430	252
KS-810	37.0	42.4	109	34.2	440	26.5	467	207
LM-2	61.0	40.4	68	36.4	544	28.9	524	267
Paranapanema rocks								
KS-624	65.0	43.6	157	36.0	354	19.0	343	177
KS-660	59.9	43.6	148	33.4	377	20.6	331	171
KS-671	54.0	42.2	191	37.0	355	27.1	347	164
KS-685	47.0	48.2	111	33.7	415	17.5	321	203
KS-703	44.1	43.8	109	37.7	412	25.3	297	189
KS-704	48.1	40.9	92	35.6	449	28.5	397	187
KS-705	51.4	43.8	158	39.3	447	25.8	386	190
KS-706	48.4	44.9	93	38.9	474	16.1	362	181
KS-707	47.2	43.9	161	44.3	458	19.9	324	189
KS-755	44.0	56.1	93	50.4	368	27.9	396	214

Sample	Cs	Hf	Nb	Ta	Th	U	Y
Pitanga rocks							
KS-616	0.32	5.6	19	1.60	3.04	0.76	37
KS-620	0.52	7.5	37	1.77	3.57	1.09	52
KS-622	0.32	7.5	24	1.82	3.60	0.82	40
KS-623	0.30	7.6	26	1.71	3.25	0.71	38
KS-625	0.32	7.6	35	2.10	3.77	0.79	45
KS-626	0.36	7.2	28	1.94	3.68	0.76	43
KS-627	0.41	7.1	27	1.78	3.47	0.68	43
KS-628	0.25	7.1	32	2.01	3.56	0.72	43
KS-630	0.22	6.6	24	1.63	3.17	0.64	41
KS-632	0.27	7.9	35	2.19	3.96	0.83	46
KS-633	0.37	6.7	23	1.72	3.37	0.80	49
KS-638	0.43	7.3	19	1.89	3.89	0.80	36
KS-649	0.25	5.9	24	1.40	2.70	0.54	50

Table 2 (*continued*)

Sample	Ni	Co	Cr	Sc	Sr	Rb	Ba	Zr
KS-658	n.d.	5.5	24	1.46	3.46	0.89	38	
KS-681	n.d.	8.5	30	1.60	3.30	0.65	48	
KS-682	0.47	7.2	36	2.00	3.66	0.76	51	
KS-683	0.45	7.5	36	1.80	3.70	0.87	55	
KS-684	0.50	5.4	26	1.41	2.70	0.56	51	
KS-695	0.20	5.5	23	1.41	2.84	0.54	36	
KS-696	n.d.	5.5	21	1.37	2.68	0.63	36	
KS-697	n.d.	5.3	21	1.28	2.60	0.48	31	
KS-698	0.17	4.7	23	1.42	2.56	0.48	39	
KS-700	0.12	5.5	21	1.41	2.86	0.65	36	
KS-701	0.13	5.5	21	1.35	2.80	0.65	34	
KS-702	n.d.	5.1	22	1.47	2.80	0.56	40	
KS-746	0.43	5.9	14	1.42	3.33	0.71	36	
KS-747	0.21	4.1	11	1.16	2.73	0.57	33	
KS-749	0.10	3.1	16	1.11	1.95	0.34	33	
KS-756	0.56	7.3	29	1.68	3.47	0.82	31	
KS-759	0.23	6.1	19	1.73	2.88	0.53	38	
KS-760	0.59	6.9	23	1.77	2.93	0.62	39	
KS-762	0.62	8.6	33	2.26	4.19	0.94	38	
KS-763	0.33	7.8	31	2.35	3.95	0.79	46	
KS-764	0.31	5.2	18	1.46	2.46	0.50	27	
KS-765	n.d.	5.5	20	1.44	2.68	0.48	27	
KS-770	0.79	7.0	23	1.81	4.76	1.21	32	
KS-772	0.40	7.7	29	2.02	3.93	0.82	32	
KS-775	n.d.	8.6	29	2.24	4.52	0.93	39	
KS-778	0.36	6.2	24	1.90	3.75	0.87	33	
KS-786	0.18	6.1	23	1.58	2.99	0.71	32	
KS-787	0.28	6.6	23	1.58	3.12	0.62	32	
KS-788	0.36	6.9	24	1.68	3.12	0.67	38	
KS-790	0.15	6.0	23	1.70	3.01	0.46	32	
KS-793	0.32	5.4	20	1.42	2.45	0.51	30	
KS-794	0.41	6.7	24	1.67	3.11	0.51	33	
KS-810	n.d.	6.1	14	1.71	3.16	0.55	33	
LM-2	1.31	5.8	22	1.77	3.58	0.67	37	
Paranapanema rocks								
KS-624	0.28	4.7	16	1.15	2.60	0.54	30	
KS-660	0.15	3.3	14	1.03	2.22	0.56	33	
KS-671	0.39	3.4	14	1.06	2.64	0.41	31	
KS-685	0.56	4.9	14	1.08	2.56	0.50	35	
KS-703	0.35	4.4	14	1.10	3.08	0.62	39	
KS-704	0.55	3.9	17	1.14	3.07	0.63	38	
KS-705	0.47	4.1	18	1.18	3.35	0.60	40	
KS-706	n.d.	4.4	16	1.14	3.06	0.55	36	
KS-707	0.57	4.5	15	1.01	2.92	0.63	39	
KS-755	0.15	6.5	13	1.22	3.16	0.63	37	

Sample	La	Ce	Nd	Sm	Eu	Tb	Yb	Lu
Pitanga rocks								
KS-616	30.98	69.45	37.61	8.86	2.76	1.27	3.33	0.45
KS-620	42.76	97.82	52.51	11.80	3.64	1.69	3.25	0.43
KS-622	37.80	80.81	40.31	9.76	2.67	1.46	3.69	0.46
KS-623	37.47	75.09	37.24	9.09	2.91	1.36	2.87	0.40
KS-625	41.99	91.08	53.71	11.05	3.30	1.59	3.91	0.55
KS-626	34.98	66.32	37.40	9.29	3.31	1.37	3.13	0.38
KS-627	36.63	83.39	43.67	9.80	3.24	1.52	3.54	0.47
KS-628	41.20	88.58	42.90	10.32	3.14	1.54	3.77	0.50
KS-630	34.16	75.21	46.66	9.98	2.88	1.48	3.97	0.49
KS-632	41.60	86.35	44.76	10.72	3.44	1.57	3.47	0.45
KS-633	33.08	66.73	35.63	9.51	3.34	1.33	3.18	0.44
KS-638	40.01	88.21	46.80	10.44	3.26	1.62	4.07	0.55
KS-649	28.00	60.00	36.35	7.82	2.50	1.30	3.40	0.45
KS-658	32.46	74.18	40.24	9.83	2.89	1.73	3.32	0.45
KS-681	38.50	83.00	48.00	9.60	3.00	1.50	3.40	0.43
KS-682	40.61	90.50	35.00	9.57	2.50	1.56	3.40	0.45
KS-683	41.00	92.00	54.00	10.50	3.50	1.70	3.20	0.48
KS-684	32.23	64.27	40.12	8.65	2.70	1.34	3.70	0.49
KS-695	27.43	65.00	37.86	8.05	2.55	1.45	2.60	0.37
KS-696	27.00	64.20	43.60	4.94	n.d.	1.35	3.88	0.44
KS-697	26.08	56.80	36.35	7.01	2.63	1.34	3.28	0.38
KS-698	26.08	59.86	37.50	7.01	2.80	1.44	3.05	0.40
KS-700	29.94	65.13	37.68	8.48	2.67	1.35	2.83	0.41
KS-701	31.10	76.30	38.80	8.22	2.76	1.20	2.53	0.38
KS-702	26.05	56.50	37.30	7.82	2.72	1.30	2.93	0.37
KS-746	31.37	67.90	33.78	7.53	2.85	1.26	3.28	0.47

(*continued on next page*)

Table 2 (*continued*)

Sample	Ni	Co	Cr	Sc	Sr	Rb	Ba	Zr
KS-747	26.01	54.19	26.69	6.19	1.85	0.92	2.60	0.39
KS-749	21.24	45.57	25.25	5.81	2.05	0.93	1.93	0.27
KS-756	34.88	73.83	42.06	9.11	n.d.	1.44	3.12	0.45
KS-759	28.41	62.29	31.81	7.50	2.51	1.38	3.67	0.48
KS-760	31.47	70.42	38.86	8.65	3.13	1.50	3.06	0.39
KS-762	41.18	93.48	50.78	10.48	3.06	1.60	3.49	0.46
KS-763	40.02	88.67	45.64	10.44	3.51	1.66	3.87	0.56
KS-764	27.16	61.02	31.03	7.30	2.33	1.17	2.85	0.40
KS-765	25.27	55.79	32.92	6.89	2.36	1.00	2.85	0.37
KS-770	43.56	93.76	46.33	10.11	3.39	1.27	3.27	0.47
KS-772	40.64	92.54	47.95	10.31	2.94	1.43	3.48	0.48
KS-775	45.96	101.89	52.55	11.62	3.67	1.79	4.34	0.56
KS-778	33.80	73.59	40.54	8.47	2.75	1.42	3.32	0.48
KS-786	31.74	71.38	38.47	8.80	2.89	1.22	2.90	0.41
KS-787	31.85	63.97	31.33	8.52	2.60	1.24	3.08	0.41
KS-788	35.56	80.54	n.d.	10.18	3.43	1.31	3.54	0.49
KS-790	30.89	68.54	35.51	8.14	2.81	1.25	3.25	0.43
KS-793	27.15	64.05	31.79	7.62	2.15	1.12	2.90	0.39
KS-794	34.85	77.98	39.51	9.60	3.14	1.36	3.50	0.48
KS-810	31.40	71.31	35.00	7.93	2.77	1.15	3.20	0.44
LM-2	37.56	82.04	41.76	8.82	2.87	1.44	3.24	0.43
Paranapanema rocks								
KS-624	24.45	53.59	28.91	6.86	2.31	1.23	3.25	0.48
KS-660	21.17	45.96	25.92	6.14	2.09	1.03	2.70	0.41
KS-671	24.23	53.38	24.71	5.78	2.24	1.02	2.89	0.39
KS-685	23.88	51.91	29.47	6.91	2.34	1.12	3.17	0.46
KS-703	24.50	61.70	26.70	6.13	2.19	1.38	3.62	0.49
KS-704	23.13	50.86	29.60	4.30	2.31	1.22	3.28	0.53
KS-705	25.40	57.70	30.27	6.60	2.16	1.42	3.60	0.48
KS-706	23.80	57.10	31.70	6.33	2.17	1.41	3.60	0.48
KS-707	27.09	66.90	32.00	3.54	2.32	1.36	3.65	0.52
KS-755	27.74	61.82	32.72	7.48	2.19	1.29	3.38	0.44

Trace element abundances expressed in μg/g. Ni, Cr, Sr, Zr, Nb, and Y by X-ray fluorescence (Instituto de Geociências e Ciências Exatas, UNESP). Remaining trace elements by instrumental neutron activation analysis (IPEN). n.d., not detected.

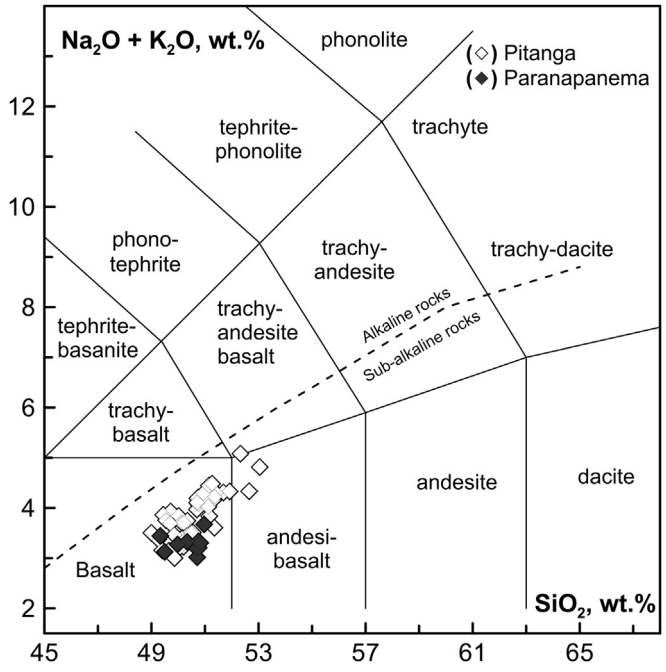

Fig. 2. Total alkali-silica (TAS) diagram (Le Bas et al., 1986; Le Bas and Streckeisen, 1991) used for the nomenclature of basic volcanic rocks of Paraná Continental Flood Basalt Province. The dividing dotted line between alkalic and sub-alkalic magma series is from Irvine and Baragar (1971).

relationship through different degrees of partial melting of a common mantle source, as can be seen in Fig. 6.

REE patterns of PCFB, normalized to chondrites (McDonough and Sun, 1995), are displayed in Fig. 7. All chondrite-normalized REE patterns (Fig. 7) are strongly enriched in LREE relative to heavy REE (HREE). Most notable is the generally parallel nature of the patterns. Differences in percentage of partial melting from a common source could explain the sloping of REE patterns for the Paranapanema [$(La/Lu)_N$ 4.5 to 6.5] when compared with those for the Pitanga [$(La/Lu)_N$ 6.1 to 10.3] types (Fig. 7). The Pitanga and Paranapanema basalts have similar $(La/Sm)_N$ ratios (2.1–3.4 and 2.2–4.8, respectively). There are no large variations in Eu anomalies in Pitanga ($Eu/Eu^* = 0.8–1.1$) and Paranapanema rocks ($Eu/Eu^* = 0.9–1.4$). The Pitanga and Paranapanema rocks show high $(La/Yb)_N$ ($= 7.0 \pm 1.0$ and 5.1 ± 0.4, respectively; 1 st. Dev.) and low Lu/Hf ($= 0.07 \pm 0.01$ and 0.11 ± 0.02, respectively; 1st. Dev.), which indicate that they likely formed by melting of a source that contained variable content of residual garnet, as has been pointed out previously (Piccirillo and Melfi, 1988).

Shown in Fig. 8 are primitive-mantle-normalized trace element diagrams (McDonough and Sun, 1995). These patterns reveal some differences between the rocks from the two magma-types. All the patterns of Pitanga and Paranapanema rocks exhibit significant enrichment in LILE, such as Ba, Rb, Th, and K, relative to some HFSE (such as Nb, Ta, Zr, Hf, Ti, and P). Compared to Paranapanema basalts, Pitanga rocks have slightly enriched patterns.

The Pitanga and Paranapanema rocks show negative Nb and Ta anomalies [$(Nb/La)_N = 0.4–0.9$ and 0.5–0.7, respectively], and have minor negative Sr and P anomalies. The negative Nb–Ta anomaly in particular has been attributed as SCLM signature in previous studies (e.g., Piccirillo and Melfi, 1988; Hawkesworth et al., 1992; Marques et al., 1999). The patterns resemble those found in subduction environments [island-arc basalts (IAB); (Fig. 8)], as well as in continental crust. The REE patterns of the investigated samples (Pitanga and Paranapanema magma type) are also similar (parallel to) to those of IAB (Fig. 7).

4.2. Strontium, neodymium, and lead isotopes

Twenty Sr, Nd, and Pb isotope analysis were carried out for Pitanga and Paranapanema tholeiitic basalts (Fig. 9; Table 3). Based on published Ar–Ar ages for Paraná basalts (e.g., Renne et al., 1992; Thiede and Vasconcelos, 2010) and U–Pb ages for Paraná felsic rocks (Janasi et al., 2011), the initial $^{87}Sr/^{86}Sr$ and $^{143}Nd^{144}Nd$ ratios are calculated to the average age of 133 Ma. Despite their generally distinct major and incompatible element compositions, the two groups have similar isotopic compositions.

In the Pitanga basalts initial $^{87}Sr/^{86}Sr$ varies from 0.70538 to 0.70642 and $\varepsilon_{Nd}(T)$ values vary from −5.6 to −2.7 ($^{143}Nd/^{144}Nd_i$: 0.51233–0.51218). These rocks show small variations in Pb isotopic compositions, where $^{206}Pb/^{204}Pb_m$ vary from 17.741 to 18.247, $^{207}Pb/^{204}Pb_m$ from 15.499 to 15.566 and $^{208}Pb/^{204}Pb_m$ from 38.183 to 38.431.

The Paranapanema rocks type have Sr, Nd, and Pb isotopic compositions very similar to Pitanga basalts. $^{87}Sr/^{86}Sr_i$ varies from 0.70552 to 0.70631 and $\varepsilon_{Nd}(T)$ values from −4.8 to −3.9 ($^{143}Nd/^{144}Nd_i$: 0.51227–0.51222). $^{206}Pb/^{204}Pb_m$ ranges from 17.887 to 18.135, $^{207}Pb/^{204}Pb_m$ from 15.513 to 15.562 and $^{208}Pb/^{204}Pb_m$ from 38.260 to 38.446.

Lead isotopic data are plotted in Fig. 9b. Data for both Pitanga and Paranapanema rocks define essentially a linear array subparallel to the North Hemisphere Reference Line (NHRL; Hart, 1984) calculated on the NHRL today, with $\Delta^{7/4} = +11.6$ to +12.7and +9.8 to +12.8 and $\Delta^{8/4} = +98.7$ to +107.0 and +98.7 to +104.0 for Pitanga and Paranapanema rocks, respectively. The $\Delta^{7/4}$ and $\Delta^{8/4}$

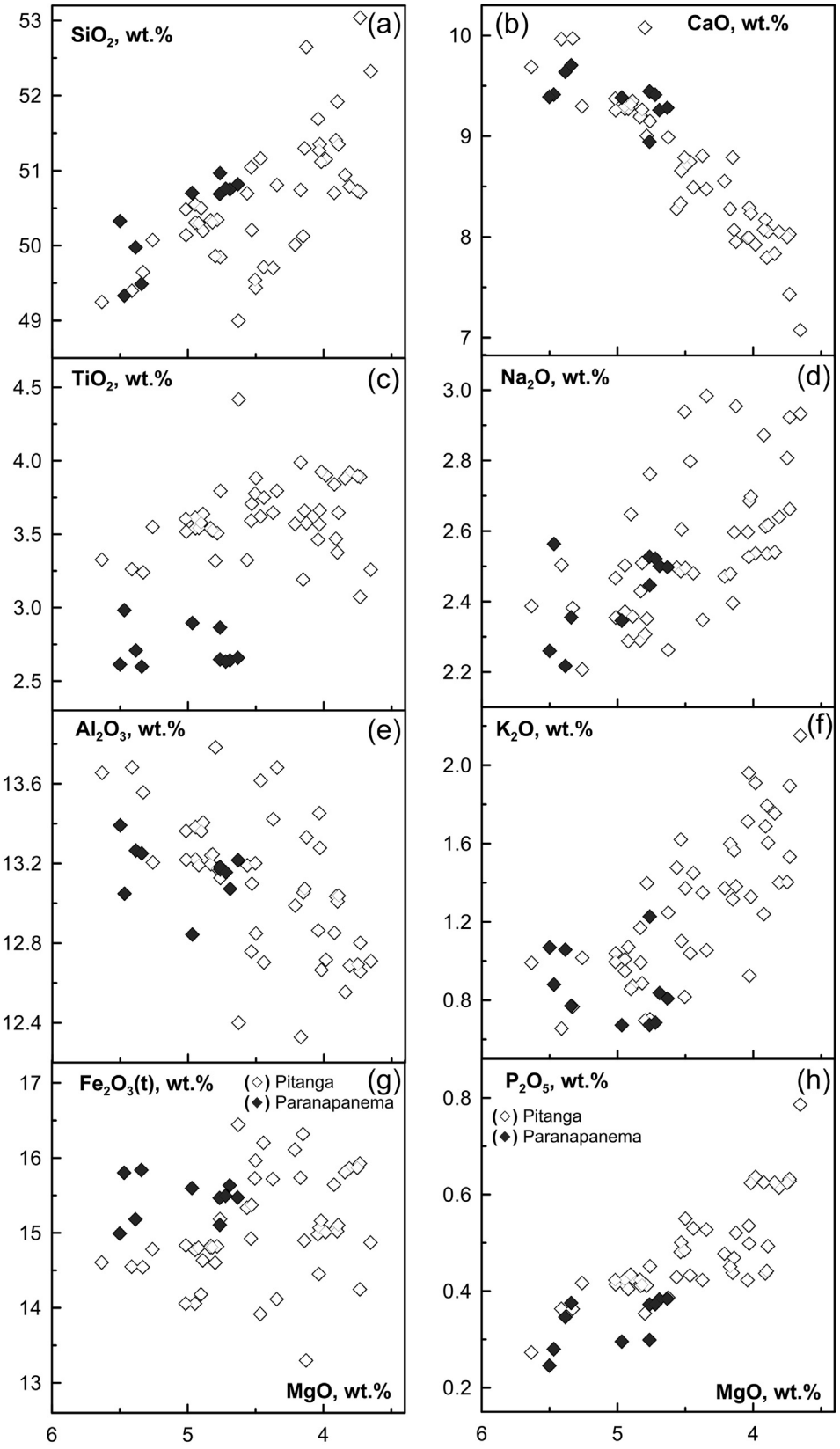

Fig. 3. MgO (wt.%) versus major and minor element (wt.%) variation diagrams for the PCFB rocks.

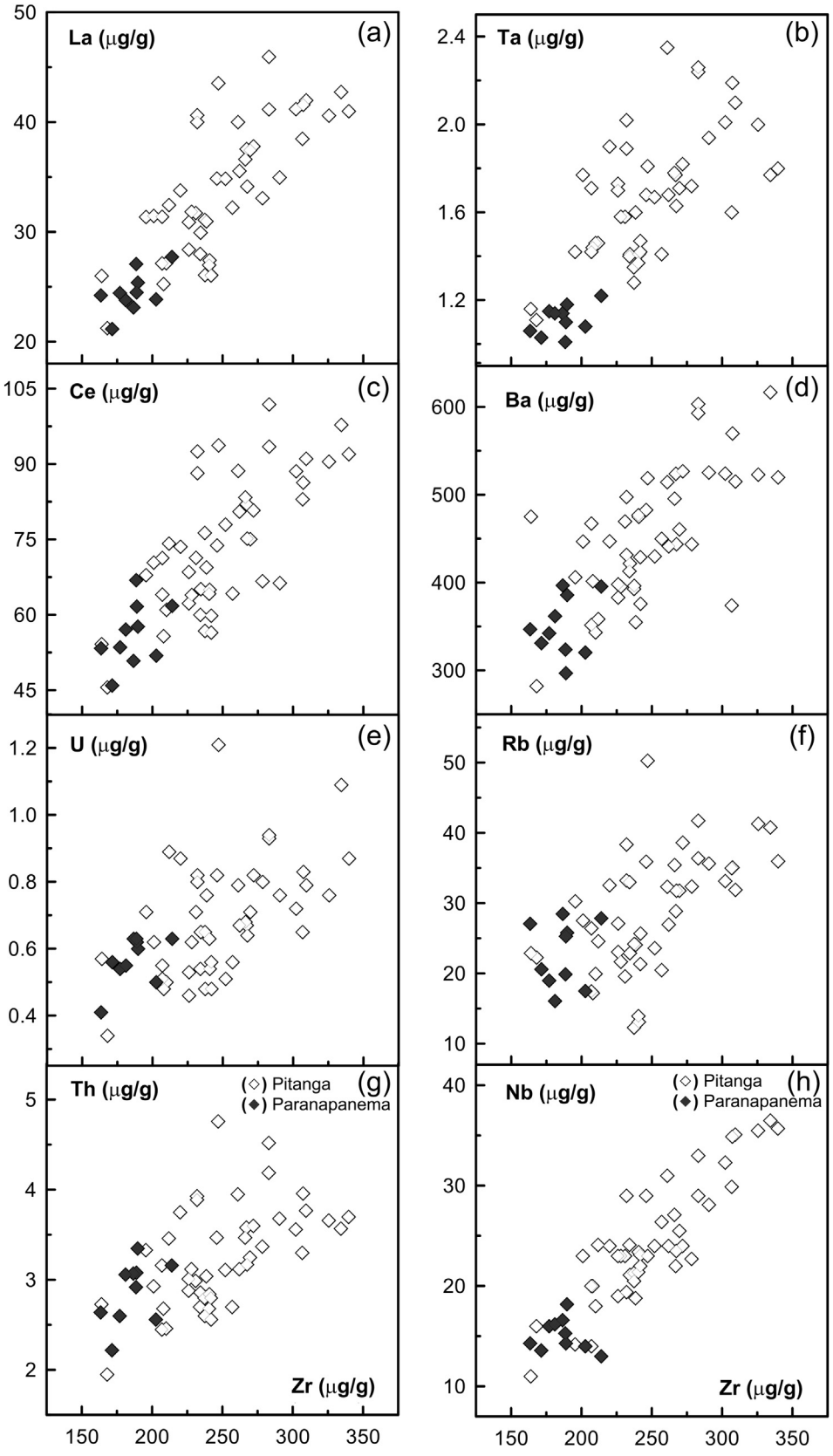

Fig. 4. Trace element variation diagrams using Zr (μg/g) as a differentiation index for the PCFB rocks.

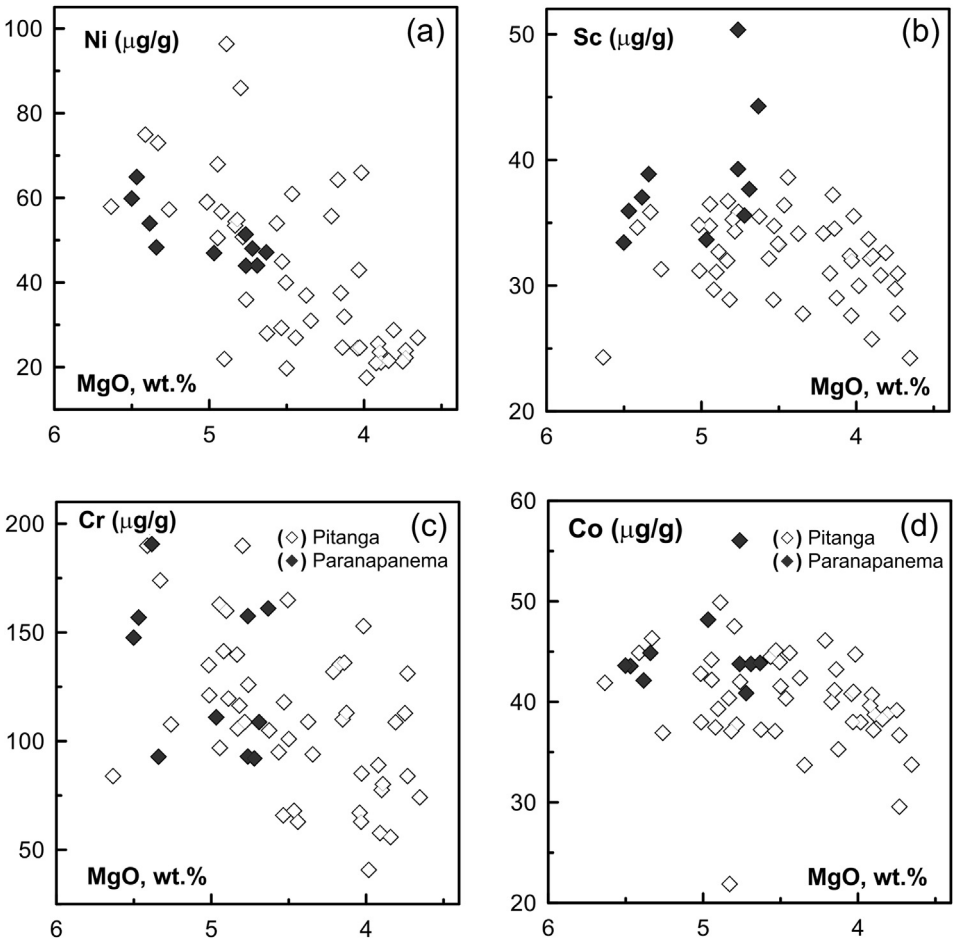

Fig. 5. MgO (wt.%) versus compatible trace element (wt.%) variation diagrams for the PCFB rocks.

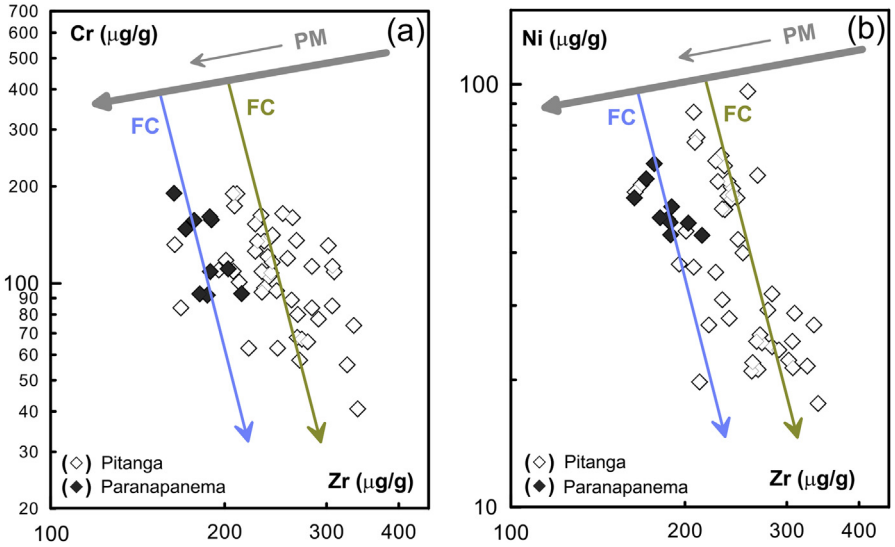

Fig. 6. (a) Zr (μg/g) versus log (Cr). (b) Zr (μg/g) versus log (Ni). These diagrams illustrate that the Pitanga and Paranapanema rocks may reflect differences in the degrees of partial melting (different depths) of a common mantle source, according to the lines drawn in the diagrams. FC = Fractional crystallization; PM = Partial melting.

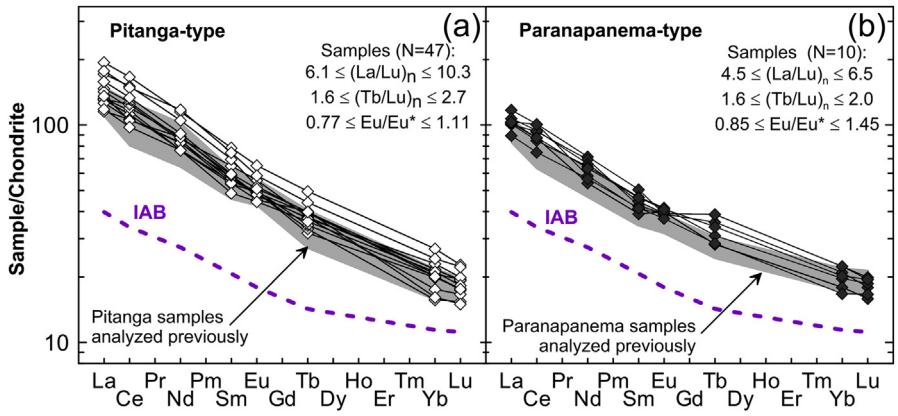

Fig. 7. Chondrite-normalized (McDonough and Sun, 1995) rare earth elements patterns for basalts from the Paraná Continental Flood Basalt Province: (a) Pitanga magma type compared to Pitanga samples analyzed previously (in others studies) and Island Arc Basalts (IAB); (b) Paranapanema magma type compared to Paranapanema samples analyzed previously (in others studies) and IAB. IAB from Kelemen et al. (2003).

represent the vertical deviation of $^{207}Pb/^{204}Pb$ and $^{208}Pb/^{204}Pb$ relative to the NHRL for a given $^{206}Pb/^{204}Pb$, as defined by Hart (1984).

5. Discussion

5.1. Crustal contamination

Before the mantle sources of these mafic parental magmas can be defined, the role of continental crustal interaction in modifying the chemical and isotopic compositions of the magmas must be discussed. Assimilation of even small amounts of felsic crustal rocks results in a sharp increase in the abundances of Ba, Pb, U, Th, and LREE, but should have little effect on the concentrations of Ta, Nb, Y, Ti, and HREE (Puchtel et al., 1998).

A particularly sensitive indicator of contamination by intermediate to felsic crust is the P_2O_5/K_2O ratio (e.g., Carlson and Hart, 1987; Hart et al., 1997) since silicic composition crustal rocks have low P_2O_5/K_2O, generally, lower than 0.1 (Fig. 10a), while mantle derived magmas typically have relatively high P_2O_5/K_2O. Decreasing P_2O_5/K_2O along with increase in $^{87}Sr/^{86}Sr$ ratios are expected for basic magmas mixing with crustal materials. This behaviour was not observed in the analyzed high-Ti basalts, which probably indicates that these rocks were not significantly affected by crustal contamination. Consistently high-Ti basalts investigated in this study do not show a positive correlation between $^{87}Sr/^{86}Sr_i$ and SiO_2 (Fig. 10b).

According to Shirey and Walker (1998) and Widom (2011), the extreme disparity in isotopic signatures between the depleted mantle and crustal materials makes the Os isotopic system a particularly sensitive tracer of crustal involvement in magma petrogenesis. In this context, based on osmium isotopic composition studies in the PCFB, Rocha-Júnior et al. (2012) demonstrated that the Pitanga and Paranapanema basalts (γ_{Os} values calculated for 133 Ma range from +1.0 to +2.0) were not affected by crustal contamination.

With respect to trace element compositions, the Pitanga and Paranapanema basalts show a strong variation of Nb/Th and Nb/La ratios from 4.0 to 0.4, respectively, to 10.2 and 0.9 [$(Nb/Th)_N$ ratios from 0.5 to 1.2; $(Nb/La)_N$ from 0.4 to 0.9] (Fig. 10). These tholeiites have similar Nb/Th and Nb/La ratios as are observed in EM-I (enriched mantle I) component ocean island basalts (e.g., Eisele et al., 2002). Variations in Nb/Th and Nb/La in mafic rocks are generally attributed to sediment assimilation in the mantle source (Weaver, 1991) or during passage through the crust. However, the basalts are homogeneous with respect to their Sr, Nd, and Pb isotopic compositions (Fig. 9) and do not display any correlation between Nb/Th or Nb/La and the Sr, Nd or Pb isotopic ratios. This requires another process than low-pressure crustal contamination to explain the geochemical characteristics.

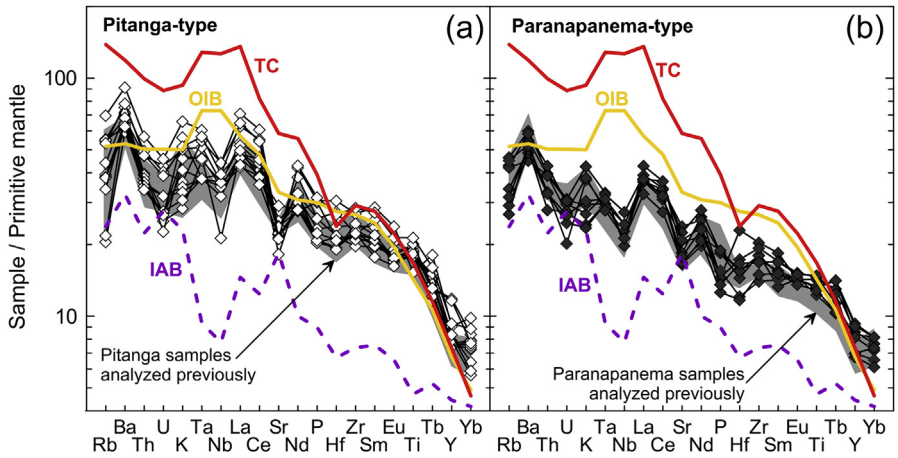

Fig. 8. Primitive-mantle normalized trace element diagram [normalizing values from McDonough and Sun (1995)]. In contrast to the PCFB, the trace element pattern of the OIBs (in particular Tristan da Cunha volcanics) shows a distinctive Nb–Ta positive anomaly. Data sources: Island Arc Basalts (IAB) from Kelemen et al. (2003); OIB and N-MORB (Sun and McDonough, 1989); Tristan da Cunha (TC) is based on data from the GEOROC database (http://georoc.mpch-mainz.gwdg.de/georoc/).

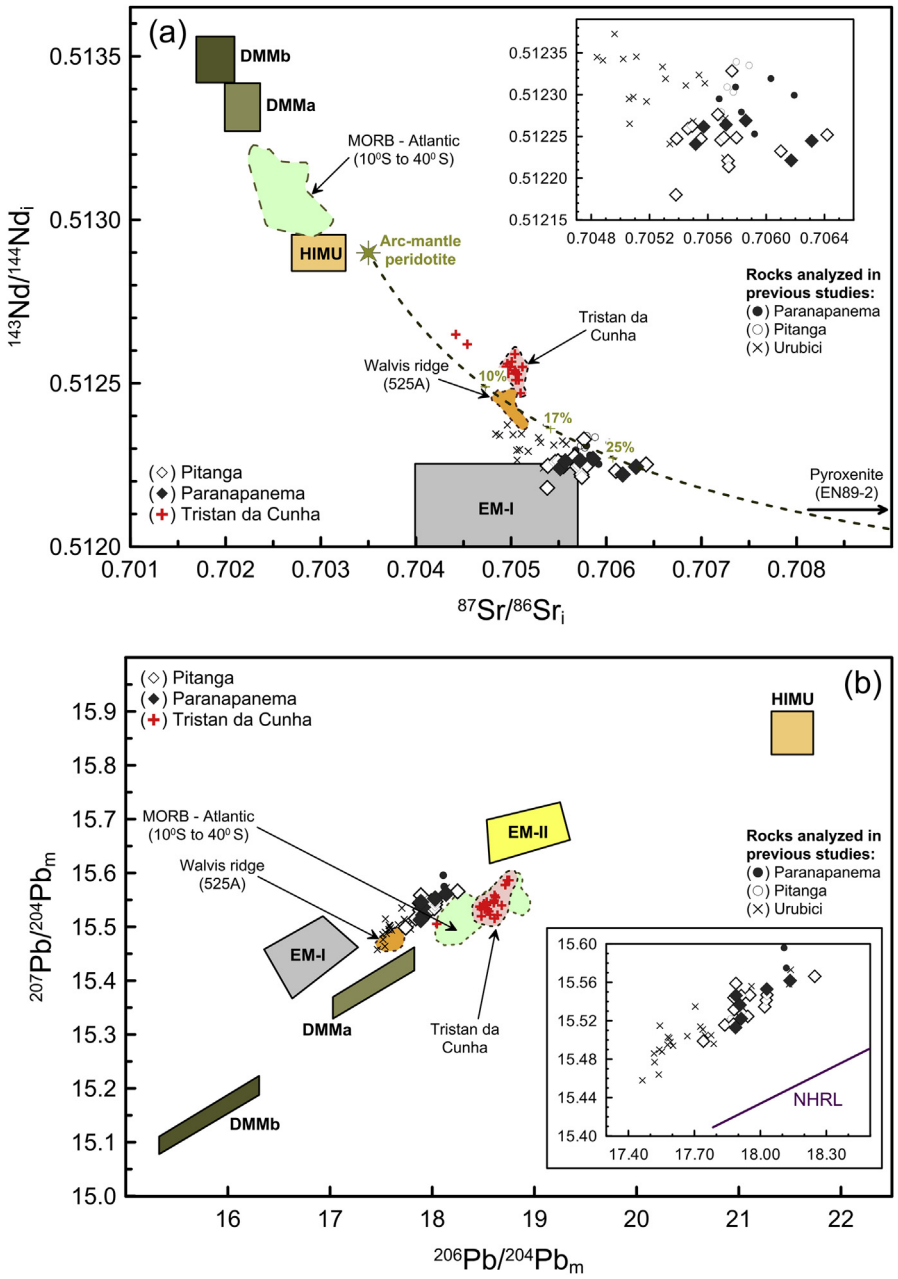

Fig. 9. (a) Initial $^{87}Sr/^{86}Sr$ (at 133 Ma) plotted against initial $^{143}Nd/^{144}Nd$. Modelling assumes two-component mixing between sublithospheric mantle (represented by arc-mantle peridotite) and a hypothetical "mafic vein" material (pyroxenite EN89-2). We consider that the pyroxenite (EN89-2) was extracted from the mantle at 1.2 Ga (with the same $^{187}Re/^{188}Os$ and $^{147}Sm/^{144}Nd$ ratios). Sublithospheric mantle ($^{87}Sr/^{86}Sr = 0.7035$, [Sr] = 12 μg/g, $^{143}Nd/^{144}Nd = 0.5129$, [Nd] = 1.2 μg/g); pyroxenite EN89-2 ($^{87}Sr/^{86}Sr = 0.70915$, [Sr] = 30 μg/g, $^{143}Nd/^{144}Nd = 0.51205$, [Nd] = 10 μg/g). (b) $^{206}Pb/^{204}Pb$ plotted against initial $^{207}Pb/^{204}Pb$. Northern Hemisphere Reference Line (NHRL; Hart, 1984). Atlantic (10°–40°S) MORB (PET-DB database; http://www.petdb.org). The parameters for the EM-I, EM-II, and HIMU are from Hofmann (2003), Jackson and Shirey (2011), and Zindler and Hart (1986). The parameters for the arc-mantle peridotite are from Handler et al. (2005), Hart et al. (1997), and Tatsumoto et al. (1992). The parameters for the pyroxenite EN89-2 are from Carlson and Irvine (1994), and Chesley et al. (2004). Tristan da Cunha (TC) is based on data from the GEOROC database (http://georoc.mpch-mainz.gwdg.de/georoc/).

5.2. Influence of subduction-related fluids and/or magmas

As noted in primitive-mantle normalized trace element diagrams (Fig. 8; McDonough and Sun, 1995), the Pitanga and Paranapanema rocks show negative Nb and Ta anomalies [$(Nb/La)_N = 0.4–0.9$ and 0.5–0.7, respectively; $(Nb/Th)_N = 0.5–1.2$ and 0.5–0.7, respectively]; the patterns resembling those found in subduction environments [island-arc basalts (IAB); $(Nb/La)_N \sim 0.5$; $(Nb/Th)_N \sim 0.4$] (Fig. 8). The depletion of Nb and Ta relative to La is not a characteristic of MORB and OIB, and together with enrichments in Sr and Nd isotopic signatures (negative ε_{Nd}) have been the basis for models invoking the SCLM in the generation of the PCFB (e.g., Piccirillo and Melfi, 1988; Hawkesworth et al., 1992; Marques et al., 1999). In particular, the incompatible trace element ratios (e.g., La/Th, Nb/La, Zr/Ta) of the PCFB tholeiites are not similar to those found in OIB and Tristan da Cunha least evolved alkaline volcanics, which can be used to assert that these components did not play a substantial role in the PCFB generation (Fig. 8). It should be noted instead that low Nb/La ratios (<1) are characteristic of subduction-related magmatism (McCulloch and Gamble, 1991).

In this way, PCFB rocks may be derived from mantle source regions that are chemically similar to the sources of IABs (e.g., Kelemen

Table 3
Sr–Nd–Pb isotopic data for Pitanga and Paranapanema rocks from northern PCFB.

Sample	$^{87}Sr/^{86}Sr$	$^{143}Nd/^{144}Nd$	$\varepsilon^{143}Nd_i$[a]	T_{DM} (Ga)	$^{206}Pb/^{204}Pb$	$^{207}Pb/^{204}Pb$	$^{208}Pb/^{204}Pb$
Pitanga rocks							
KS-625	0.706048 ± 50	0.512384 ± 8	−3.7	1.13	17.943 ± 7	15.525 ± 7	38.341 ± 8
KS-649	0.706221 ± 64	0.512362 ± 10	−4.3	1.24	17.953 ± 4	15.547 ± 4	38.395 ± 10
KS-684	0.705790 ± 70	0.512361 ± 9	−4.3	1.25	17.880 ± 5	15.544 ± 5	38.387 ± 12
KS-695	0.706225 ± 41	0.512344 ± 10	−4.6	1.25	17.889 ± 27	15.559 ± 24	38.366 ± 64
KS-700[b]	0.705650 ± 95	0.512359 ± 10	−4.3	1.23	17.882 ± 3	15.532 ± 2	38.326 ± 7
KS-701	0.705834 ± 51	0.512357 ± 10	−4.3	1.23	17.878 ± 1	15.516 ± 1	38.304 ± 2
KS-746	0.706225 ± 48	0.512331 ± 10	−4.9	1.36	18.030 ± 11	15.547 ± 11	38.389 ± 11
KS-747	0.706082 ± 39	0.512343 ± 7	−4.8	1.43	18.027 ± 8	15.542 ± 8	38.362 ± 8
KS-749	0.705655 ± 55	0.512301 ± 8	−5.6	1.48	17.741 ± 7	15.499 ± 7	38.183 ± 7
KS-756	0.706162 ± 82	0.512442 ± 8	−2.7	1.12	18.247 ± 11	15.566 ± 12	38.431 ± 13
KS-772	0.706120 ± 85	0.512362 ± 5	−4.3	1.24	18.020 ± 9	15.535 ± 8	38.380 ± 9
KS-775	0.706014 ± 49	0.512378 ± 5	−4.0	1.26	17.839 ± 9	15.516 ± 8	38.268 ± 8
KS-778	0.705956 ± 98	0.512369 ± 7	−4.0	1.18	17.920 ± 7	15.527 ± 7	38.341 ± 7
LM-2	0.706708 ± 57	0.512363 ± 4	−4.2	1.21	17.913 ± 8	15.546 ± 7	38.394 ± 8
Paranapanema rocks							
KS-624[b]	0.706018 ± 72	0.512382 ± 8	−4.0	1.28	17.889 ± 1	15.546 ± 1	38.369 ± 3
KS-660[b]	0.706159 ± 50	0.512385 ± 11	−3.9	1.25	17.887 ± 4	15.513 ± 4	38.260 ± 9
KS-671	0.706590 ± 49	0.512344 ± 3	−4.8	1.45	18.029 ± 7	15.553 ± 6	38.421 ± 6
KS-685[b]	0.705801 ± 41	0.512379 ± 10	−4.0	1.27	17.907 ± 4	15.537 ± 3	38.341 ± 8
KS-705	0.706628 ± 46	0.512360 ± 10	−4.3	1.27	18.135 ± 10	15.562 ± 11	38.446 ± 11
KS-755	0.705931 ± 47	0.512361 ± 8	−4.4	1.36	17.913 ± 8	15.522 ± 7	38.300 ± 7

[a] Calculated for the age of 133 Ma.
[b] These isotopic compositions were determined by Rocha-Júnior et al. (2012).

et al., 2003), although caution should be taken for this conclusion. In short, the main evidence for the involvement of metasomatic components, possibly related to supra-subduction environments, in the source of the PCFB includes: (1) enrichment of LREE relative to HREE (Fig. 7), (2) enrichment in mobile LILE (Figs. 7 and 8), and (3) strong negative anomalies of Nb–Ta (Fig. 8). Thereby, we propose that the northern high-Ti PCFB source is the sublithospheric mantle affected by fluids and/or magmas related to subduction.

Bologna et al. (2013) discuss the existence of a major lithospheric discontinuity on the western Paraná Basin. An eastward dipping electrical and density variation within the crust and upper mantle could be remnant of an ancient subduction of an oceanic lithosphere and the closure of the Clymenes ocean (Tohver et al., 2010) in Cambrian times. This major tectonic process brought together the Rio Apa terrain, the inversion of marginal basins (Paraguay fold/thrust belt) and the final amalgamation of the Paraná terrains. As a result, the mantle wedge, above the subducted oceanic lithosphere, may have been frozen and coupled to the base of the Parana basin lithospheric plate above which the Paleozoic subsidence and subsequent Early Cretaceous magmatism occurred.

5.3. Relationships between PCFB source and alkaline magmatism that surround the Paraná Basin

The emplacement of alkaline and alkaline–carbonatitic complexes in and around the PCFB occurred mainly along tectonic lineaments active at least since the Early Mesozoic (e.g., Comin-Chiaromonti and Gomes, 2005; Comin-Chiaramonti et al., 2007), and these alkaline rocks are distributed mainly along mobile belts (Brasiliano cycle) at the margins of the intracratonic Paraná Basin.

The Pitanga and Paranapanema tholeiites exhibit similar isotopic ratios, consistent with the presence of a regional mantle isotope signature. Note that the low Pb, low ε_{Nd}, and high Sr isotopic ratios of the high-Ti PCFB tholeiites are broadly similar to those of the Jacupiranga carbonatite (130 Ma; Huang et al., 1995), and high-Ti mafic-alkalic rocks of subsequent alkali magmatism (with an age range between 90 and 55 Ma; Gibson et al., 1995; Thompson et al., 1998), which are found on the northern and western margins of the Paraná Basin, as well as in basalts of the Walvis Ridge and Rio Grande Rise (Richardson et al., 1982; Gibson et al., 2005; Salters et al., 2010). Such compositions are different from that of North Atlantic OIB and MORB (Hofmann, 2003), and these distinct characteristics have been termed as DUPAL anomaly (Hart, 1984) and it appears to be present in basalts from both oceanic (e.g., Walvis Ridge; Enriched MORB (E-MORB) from the 48.5°–49.2° S ridge segment) and continental areas, including the high-Ti PCFB basalts (Escrig et al., 2005; Hawkesworth et al., 1986). Another feature that deserves mention is the initial γ_{Os} values for the high-Ti basalts of northern PCFB (γ_{Os} calculated for 133 Ma range from +1.0 to +2.0) which overlap the compositions of fertile SCLM xenoliths from the spatially associate Goiás Alkaline Province (γ_{Os} calculated for 85 Ma range from −5.1 to +2.2; Carlson et al., 2007). These isotopic similarities are indicative that their source(s) might be physically continuous.

The sources of the high-Ti basalts of northern PCFB, and shallower alkaline rocks at Coromandel (associated with the Alto Paranaíba arch), and high-Ti mafic-alkalic magmas of subsequent alkaline magmatism that surround the Paraná Basin, as well as some oceanic basalts with DUPAL signatures in the South Atlantic, all appear to be related to the EM-I component (Toyoda et al., 1994; Bizzi et al., 1995). Bizzi et al. (1995) and Carlson et al. (1996) emphasized that these similarities suggest some common geochemical processes associated with the formation and evolution of mobile belts around cratons that produce continental lithosphere with the general characteristics of the EM-I component of oceanic volcanism. As discussed by Bizzi et al. (1995), the oceanic basalts with DUPAL signatures in the South Atlantic are ascribed to processes by which Brazilian Neoproterozoic continental lithosphere was delaminated, and contaminated a zone of the South Atlantic asthenosphere which is now erupting as hotspot island and nearby sections of Mid-Atlantic ridge (Hawkesworth et al., 1986). According to this model, the Walvis Ridge basalts are mixtures of delaminated enriched subcontinental lithosphere and more typical "normal" oceanic compositions lying within the oceanic mantle array. Note that Gibson et al. (2005) and Peate et al. (1999) suggested a model of generation of the EM-I-like source materials, in which the present-day Tristan da Cunha plume contains a delaminated SCLM component that has undergone deep mantle

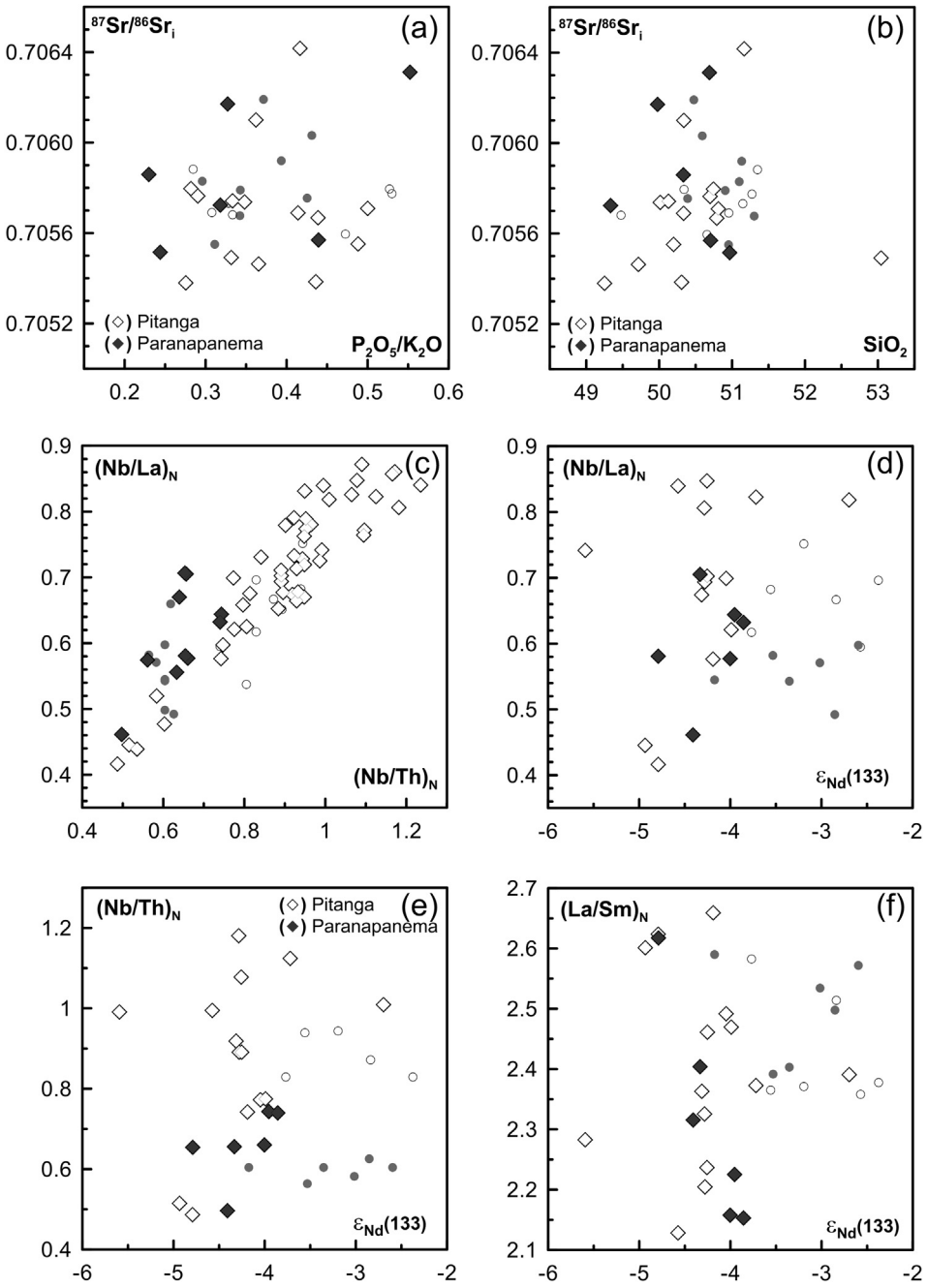

Fig. 10. Plots of (a) P_2O_5/K_2O versus $^{87}Sr/^{86}Sr_i$; (b) SiO_2 versus $^{87}Sr/^{86}Sr_i$; (c) $(Nb/Th)_N$ versus $(Nb/La)_N$; (d) $\varepsilon_{Nd}(133)$ versus $(Nb/La)_N$; (e) $\varepsilon_{Nd}(133)$ versus $(Nb/Th)_N$; (f) $\varepsilon_{Nd}(133)$ versus $(La/Sm)_N$; Pitanga (open circle) and Paranapanema (solid circle) samples analyzed previously are also shown.

recycling. Nevertheless, the supra-chondritic nature of the Tristan da Cunha basalts (initial γ_{Os} values range from +15 to +80; Rocha-Júnior et al., 2012) is contrary to evidence for an ancient SCLM component, which would have had negative initial γ_{Os} values.

In this context, we interpret that the trace element data imply that the source for the Pitanga and Paranapanema magma-types of the PCFB was mantle that had been metasomatized by slab-derived fluids. The age of this metasomatism cannot be resolved on basis of the trace element data and from Sr, Pb, and Os isotopes, but the Nd model ages (calculated in relation to the depleted mantle; T_{DM} from 1.1 to 1.4 Ga) are suggestive of a mid- to late-Proterozoic event such as the Brasiliano. Nd model ages vary from 0.8 to 1.1 Ga for the Goiás Alkaline Province and from 0.8 to 1.2 Ga for the Alto Paranaíba Igneous Province (Bizzi et al., 1995; Carlson et al., 1996, 2007; Comin-Chiaramonti et al., 2007). The Goiás Magmatic Arc (juvenile rocks), which constitutes one of the most important components of the Neoproterozoic Brasília Belt in central Brazil (northeastern Paraná basin), also has Nd model ages values mostly between 0.8 and 1.2 Ga (Pimentel et al., 2000; Laux et al., 2005). According to Valeriano et al. (2008), the Brasília Belt comprises terranes that were tectonically transported towards the western passive margin of the São Francisco – Congo palaeocontinent during an orogenic episode resulting from collision of the Paranapanema and Goiás blocks and the Goiás magmatic arc against São Francisco – Congo at 0.64–0.61 Ga. The isotopic and/or temporal overlapping of different igneous rocks cannot be accidental

and points to sampling of reservoirs formed at the same time from the same sublithospheric mantle. As a result, the metasomatized mantle can represent sublithospheric mantle metasomatized during the Neoproterozoic subduction processes (events of the Brasiliano/Pan-African orogenic cycle), which dominates the Nd, Pb, and possibly Sr isotopic compositions. To characterize this mantle region (source), we consider that the asthenospheric mantle (similar to DMM component) was enriched by fluids and/or magmas related to the Neoproterozoic subduction processes, which gave rise to Gondwanaland. This sublithospheric mantle region may have been frozen and coupled to the base of the basement of the Paraná Basin. This frozen region may be the source of the northern part (high-Ti suite) of the PCFB. This subduction-derived fluids and/or magmas might be present in the area of PCFB source given the geologic history of this region.

5.4. Mixing systematics

It has been proposed that the subduction of oceanic crust and delamination of dense mafic cumulates from the base of the continental crust are probably the most important mechanisms for recycling mafic rocks into the mantle, causing mantle heterogeneities (e.g., Hofmann, 2003; Yaxley and Green, 1998; Yaxley, 2000; see also references therein). Mafic magmatism on Earth is primarily derived from melting of mantle peridotite, even though there has been a growing consensus that multiple mantle components contribute to the production of many intraplate and some MORB and OIB magmas (Hofmann, 2003, and references therein).

Experimental petrology (Yaxley and Green, 1998; Yaxley, 2000) has been used to argue that pyroxenite or eclogite are important constituents in the source regions of some OIBs and flood basalt provinces. Pyroxenite and eclogite might be generated by hybridizing mantle peridotite with recycled components (Sobolev et al., 2005, 2007), or via high-temperature intramantle metasomatism. Moreover, Edwards (1990) suggested that the ortho- and clinopyroxenites found in mantle xenoliths and ophiolite sections are products of the fractionation sequence olivine-orthopyroxene-clinopyroxene from Mg-rich melts.

According to Yaxley (2000), a series of progressive mixing and reactions processes might re-homogenize the eclogitic component back into the peridotitic mantle, producing hybrid, re-fertilized peridotite, which may, on chemical and isotopic standpoint, constitute a suitable source for the genesis of flood basalts and OIBs. Because mafic components in the mantle (e.g., pyroxenites or eclogites) have lower solidus temperatures than those of peridotites, low-degree partial melts will preferentially sample such components (Yaxley and Green, 1998). According to those authors, eclogite will be sufficiently permeable (at 10–15% partial melting) to allow melt extraction and infiltration into surrounding peridotite, generating a metasomatized orthopyroxene-rich peridotite. Metasomatic reactions may generate a hybridized pyroxenite with nearly uniform chemical and isotopic composition (Day et al., 2009), which would constitute a single mixing end-member for the northern PCFB.

In this way, we modelled a mixing process affecting sublithospheric mantle region (peridotite end-member). As discussed by Rocha-Júnior et al. (2012), the chosen peridotite end-member has Os concentration reduced to 2 ng/g (Os concentrations similar to peridotite xenoliths of the Goiás Alkaline Province; Carlson et al., 2007), Nd increased to 1.2 μg/g with $^{143}Nd/^{144}Nd = 0.5129$ to approximate the average composition of arc-mantle peridotite xenoliths, similar to that proposed by Hart et al. (1997). The $^{187}Os/^{188}Os$ isotopic composition of this end-member was taken as the average values obtained in peridotite xenoliths of the Goiás Alkaline Province and was projected to the age of the PCFB magmatism (133 Ma). Sr compositions were taken the average values obtained in spinel peridotite xenoliths analyzed by Handler et al. (2005). The contaminant is assumed to be a hypothetical "mafic vein" material (pyroxenite EN89-2; Carlson and Irvine, 1994; Chesley et al., 2004). We consider that the pyroxenite was extracted from the mantle at 1.2 Ga (similar to Nd model ages of the PCFB and alkaline rocks that surround the Paraná Basin) and has $^{187}Re/^{188}Os$

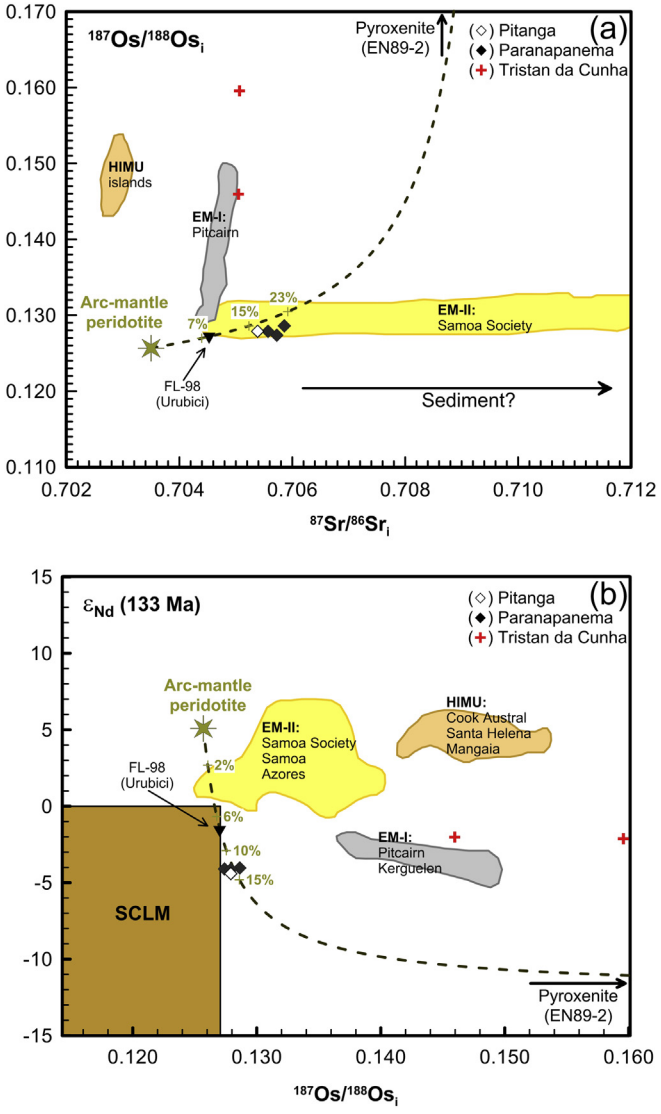

Fig. 11. (a) Initial $^{87}Sr/^{86}Sr$ (at 131.6 Ma) plotted against initial $^{187}Os/^{188}Os$. (b) $^{187}Os/^{188}Os$ plotted against initial ε_{Nd}. Modelling assumes two-component mixing between sublithospheric mantle (represented by arc-mantle peridotite) and a hypothetical "mafic vein" material (pyroxenite EN89-2). We consider that the pyroxenite (EN89-2) was extracted from the mantle at 1.2 Ga (with the same $^{187}Re/^{188}Os$ and $^{147}Sm/^{144}Nd$ ratios). Sublithospheric mantle ($^{87}Sr/^{86}Sr = 0.7035$, [Sr] = 12 μg/g, $^{143}Nd/^{144}Nd = 0.5129$ ($\varepsilon Nd = +5.1$), [Nd] = 1.2 μg/g, $^{187}Os/^{188}Os = 0.1257$, [Os] = 2 ng/g); pyroxenite EN89-2 ($^{87}Sr/^{86}Sr = 0.70915$, [Sr] = 30 μg/g, $^{143}Nd/^{144}Nd = 0.51205$, [Nd] = 10 μg/g, $^{187}Os/^{188}Os = 0.19429$, [Os] = 0.5 ng/g). The parameters for the EM-I, EM-II, HIMU, and SCLM are from Hofmann (2003), Jackson and Shirey (2011), Shirey and Walker (1998), Walker et al. (2002), and Zindler and Hart (1986). The parameters for the arc-mantle peridotite are from Handler et al. (2005), Hart et al. (1997), and Tatsumoto et al. (1992). The parameters for the pyroxenite EN89-2 are from Carlson and Irvine (1994), and Chesley et al. (2004). Tristan da Cunha (TC) is based on data from the GEOROC database (http://georoc.mpch-mainz.gwdg.de/georoc/). The osmium isotopic compositions for the Tristan da Cunha Island and Paraná rocks (Pitanga and Paranapanema) are from Rocha-Júnior et al. (2012). Figure modified after Rocha-Júnior et al. (2012).

and $^{147}Sm/^{144}Nd$ ratios as EN89-2 (Carlson and Irvine, 1994; Chesley et al., 2004).

Our models suggest that mixing 15–25% of pyroxenite (represented by EN89-2) with arc-mantle peridotite accounts for most of the isotopic systematic of the Pitanga and Paranapanema basalts (Figs. 9 and 11). Note that in an effort to minimize crustal contamination effects, only high-Ti tholeiites with initial $^{87}Sr/^{86}Sr$ lower than 0.7060 were considered to characterize the mantle source.

EM-I 'flavour' is one of the most enigmatic aspects of modern isotopic topology. Possible mechanisms for EM-I signature invokes the presence of the following recycled material in the source: delaminated SCLM (metasomatized) or mantle with recycled lower continental crust (Hauri and Hart, 1993; Shirey and Walker, 1998), oceanic crust with pelagic sediment (Rehkämper and Hofmann, 1997), subducted oceanic plateaus (Gasperini et al., 2000) and, more recently, mixtures of eclogites or pyroxenite with peridotite, or amphibole veins in the oceanic lithosphere (Yaxley and Green, 1998; Yaxley, 2000; Sobolev et al., 2005, 2007; Pilet et al., 2008; Day et al., 2009). As shown by the preceding discussion, the sources of the high-Ti basalts of the PCFB, as well as alkaline rocks that surround the Paraná Basin and oceanic basalts with DUPAL signatures appear to be related to EM-I component. Our favoured explanation is that the EM-I 'flavour' associated to these magmatic events derived from mixtures of eclogites or pyroxenite with peridotite, since pyroxenite melts freeze and react entirely with the ambient peridotite.

6. Conclusion

Our new geochemical and isotopic data, together with osmium isotopic data (Rocha-Júnior et al., 2012), for the PCFB indicate that the high-Ti basalts were derived from magmas that originated from a sublithospheric source metasomatized by pyroxenite (represented by EN89-2). The mantle source was enriched by fluids and/or magmas related to the Neoproterozoic subduction process (hybridizing mantle peridotite with recycled components), and the sublithospheric mantle may has been frozen and coupled to the base of the Paraná basin lithospheric plate above which the Paleozoic subsidence and subsequent Early Cretaceous magmatism occurred. This model is corroborated by electromagnetic soundings of the crust and upper mantle underlying the Paraná Basin (Bologna et al., 2013), whose results reveal that the basement of the Paraná Basin is a collage of several heterogeneous terranes and of lithospheric-scale suture zones.

However, what was the triggering mechanism for the mantle source melting? The Tristan da Cunha plume hypothesis has been disputed by Ernesto et al. (2002) based on paleomagnetic reconstructions. In addition, Rocha-Júnior et al. (2012) showed that the osmium isotopic data provide no evidence for the participation of Tristan da Cunha plume in the genesis of the PCFB. In that case, the mechanism of generation of the PCFB magmatism may be attributed to local hotter mantle conditions due to the combined effects of edge-driven convection (King and Anderson, 1998) and large-scale mantle warming (Coltice et al., 2007) under the Pangea supercontinent. The proximity of the PCFB magmatism to the craton margins (e.g., São Francisco, Congo, Rio de la Plata, Amazon) are consistent with the "edge-effect" mantle flow model, where the small-scale flow is driven by a discontinuity in the thickness of the lithosphere.

Acknowledgements

We would like to dedicate this contribution to our long-time, and now departed, friend E.M. (Enzo) Piccirillo. His scientific contributions to our understanding of continental flood basalts, particularly as it relates to Paraná magmatism, have been enormous. Andrea Marzoli and an anonymous reviewer are thanked for constructive reviews that helped to improve the manuscript. This study was supported by FAPESP, CNPq and CAPES (PNPD program) Brazilian agencies. These sources of support are gratefully acknowledged.

References

Anderson, D.L., 2005. Large igneous provinces, delamination, and fertile mantle. Elements 1, 271–275.
Babinski, M., Van Schumus, W.R., Chemale Jr., F., 1999. Pb–Pb dating and Pb isotope geochemistry of Neoproterozoic carbonate rocks from the São Francisco basin, Brazil: implications for the mobility of Pb isotopes during tectonism and metamorphism. Chemical Geology 160, 175–199.
Bellieni, G., Comin-Chiaramonti, P., Marques, L.S., Melfi, A.J., Nardy, A.J.R., Piccirilo, E.M., Roisenberg, A., 1984. High- and low-TiO_2 flood basalts from the Paraná plateau (Brazil): petrology and geochemical aspects bearing on their mantle origin. Neues Jahrbuch für Mineralogie 150, 273–306.
Bizzi, L.A., De Wit, M.J., Smith, C.B., McDonald, I., Armstrong, R.A., 1995. Heterogeneous enriched mantle materials and Dupal-type magmatism along the SW margin of the São Francisco craton, Brazil. Journal of Geodynamics 20 (4), 469–491.
Bologna, M.S., Ussami, N., Padua, M.B., Padilha, A.L., Vitorello, I., Fisseha, S., 2013. Mapping lithospheric sutures and amalgamated terranes within the Paraná basin integrating electromagnetic induction and gravity data. Journal of South American Earth Sciences (submitted for publication).
Carlson, R.W., Hart, W.K., 1987. Crustal genesis on the Oregon Plateau. Journal of Geophysical Research 92, 6191–6206.
Carlson, R.W., Irving, A.J., 1994. Depletion and enrichment history of subcontinental and lithospheric mantle: an Os, Sr, Nd and Pb isotopic study from the northwestern Wyoming Craton. Earth and Planetary Science Letters 126, 457–472.
Carlson, R.W., Esperança, S., Svisero, D.P., 1996. Chemical and Os isotopic study of Cretaceous potassic rocks from Southern Brazil. Contributions to Mineralogy and Petrology 125, 393–405.
Carlson, R.W., Araujo, A.L.N., Junqueira-Brod, T.C., et al., 2007. Chemical and isotopic relationships between peridotite xenoliths and mafic-ultrapotassic rocks from Southern Brazil. Chemical Geology 242, 415–434.
Chesley, J.T., Righter, K., Ruiz, J., 2004. Large-scale mantle metasomatism: a Re/Os perspective. Earth and Planetary Science Letters 219 (1–2), 49–60.
Coltice, N., Phillips, B.R., Bertrand, H., Ricard, Y., Rey, P., 2007. Global warming of the mantle at the origin of flood basalts over supercontinents. Geology 35 (5), 391–394.
Comin-Chiaramonti, P., Gomes, C.B., 2005. Mesozoic to Cenozoic Alkaline Magmatism in the Brazilian Platform. Edusp/Fapesp. São Paulo, Brazil, p. 752.
Comin-Chiaramont, P., Gomes, C.B., Cundari, A., Castorina, F., Censi, P., 2007. A review of carbonatitic magmatism in the Paraná-Angola-Namibia (PAN) system. Periodico di Mineralogia 76 (2–3), 25–78.
Cordani, U.G., Brito-Neves, B.B., D'Agrella-Filho, M.S., 2003. From Rodinia to Gondwana: a review of the available evidence from South America. Gondwana Research 6 (2), 275–283.
Day, J.M.D., Pearson, D.G., Macpherson, C.G., Lowry, D., Carracedo, J.-C., 2009. Pyroxenite-rich mantle formed by recycled oceanic lithosphere: oxygen-osmium isotope evidence from Canary Island lavas. Geology 37 (6), 555–558.
Deckart, K., Féraud, G., Marques, L.S., Bertrand, H., 1998. New time constraints on dyke swarms related to the Paraná-Etendeka magmatic province, and subsequent South Atlantic opening, southeastern Brazil. Journal of Volcanology and Geothermal Research 80, 67–83.
Edwards, S.J., 1990. Harzburgites and refractory melts in the Lewis Hills massif, Bay of Islands ophiolite complex: the base-metals and precious-metals story. Canadian Mineralogist 28, 537–552.
Eisele, J., Sharma, M., Galer, S.J.G., Blichert-Toft, J., Devey, C.W., Hofmann, A.W., 2002. The role of sediment recycling in EM-1 inferred from Os, Pb, Hf, Nd, Sr isotope and trace element systematics of the Pitcairn hotspot. Earth and Planetary Science Letters 196, 197–212.
Ernesto, M., Marques, L.S., Piccirillo, E.M., Molina, E.C., Ussami, N., Comin-Chiaramonti, P., Bellieni, G., 2002. Paraná Magmatic Province-Tristan da Cunha plume system: fixed versus mobile plume, petrogenetic considerations and alternative heat sources. Journal of Volcanology and Geothermal Research 118, 15–36.
Escrig, S., Schiano, P., Schilling, J.G., Allègre, C., 2005. Rhenium-osmium isotope systematics in MORB from the Southern Mid-Atlantic Ridge (40°–50° S). Earth and Planetary Science Letters 235, 528–548.
Ewart, A., Milner, S.C., Armstrong, R.A., Duncan, A.R., 1998. Etendeka volcanism of the Goboboseb Mountains and Messum Igneous Complex, Namibia. Part I: geochemical evidence of Early Cretaceous Tristan plume melts and the role of crustal contamination in the Paraná-Etendeka CFB. Journal of Petrology 39 (2), 191–225.
Gasperini, D., Blichert-Toft, J., Bosch, D., DelMoro, A., Macera, D., Télouk, P., Albarède, F., 2000. Evidence from Sardinian basalt geochemistry for recycling of plume heads into the Earth's mantle. Nature 408, 701–704.

Gibson, S.A., Thompson, R.N., Dickin, A.P., Leonardos, O.H., 1995. High-Ti and low-Ti mafic potassic magmas: key to plume-lithosphere interactions and continental flood-basalt genesis. Earth and Planetary Science Letters 136, 149–165.

Gibson, S.A., Thompson, R.N., Weska, R.K., Dickin, A.P., Leonardos, O.H., 1997. Late Cretaceous rift-related upwelling and melting of the Trindade starting mantle plume head beneath western Brazil. Contributions to Mineralogy and Petrology 126, 303–314.

Gibson, S.A., Thompson, R.N., Leonardos, O.H., Dickin, A.P., Mitchell, J.G., 1999. The limited extent of plume-lithosphere interactions during continental flood-basalt genesis: geochemical evidence from Cretaceous magmatism in southern Brazil. Contributions to Mineralogy and Petrology 137, 147–169.

Gibson, S.A., Thompson, R.N., Day, J.A., Humphris, S.E., Dickin, A.P., 2005. Melt-generation processes associated with the Tristan mantle plume: constraints on the origin of EM-I. Earth and Planetary Science Letters 237, 744–767.

Handler, M.R., Bennett, V.C., Carlson, R.W., 2005. Nd, Sr and Os isotope systematics in young, fertile spinel peridotite xenoliths from northern Queensland, Australia: a unique view of depleted MORB mantle? Geochimica et Cosmochimica Acta 69 (24), 5747–5763.

Hart, S.R., 1984. A large-scale isotope anomaly in the southern hemisphere mantle. Nature 309, 753–757.

Hart, W.K., Carlson, R.W., Shirey, S.B., 1997. Radiogenic Os in primitive basalts from the northwestern U.S.A.: implications for petrogenesis. Earth and Planetary Science Letters 150, 103–116.

Hauri, E.H., Hart, S.R., 1993. Re-Os isotope systematics of HIMU and EMII oceanic island basalts from the south Pacific Ocean. Earth and Planetary Science Letters 114, 353–371.

Hawkesworth, C.J., Mantovani, M.S.M., Taylor, P.N., Palacz, Z., 1986. Evidence from the Parana of South Brazil for a continental contribution to Dupal basalts. Nature 322, 356–359.

Hawkesworth, C.J., Gallager, K., Kelley, S., Mantovani, M.S.M., Peate, D., Regelous, M., Rogers, N., 1992. Paraná magmatism and the opening of the South Atlantic. In: Storey, B., Alabaster, A., Pankhurst, R. (Eds.), Magmatism and the Causes of Continental Break-up. Geological Society Special Publication, vol. 68, pp. 221–240. London.

Hofmann, A.W., 2003. Sampling mantle heterogeneity through oceanic Basalts: isotopes and trace elements. In: Carlson, R.W. (Ed.), Treatise on Geochemistry. Geochemistry of the Mantle and Core, vol. 2. Elsevier, pp. 61–101.

Huang, Y.-M., Hawkesworth, C.J., van Calsteren, P., McDermott, F., 1995. Geochemical characteristics and origin of the Jacupiranga carbonatites, Brazil. Chemical Geology 119, 79–99.

Irvine, T.N., Baragar, W.R.A., 1971. A guide to the chemical classification of the common volcanic rocks. Canadian Journal of Earth Sciences 8, 523–548.

Jackson, M.G., Shirey, S.B., 2011. Re-Os isotope systematics in Samoan shield lavas and the use of Os-isotopes in olivine phenocrysts to determine primary magmatic compositions. Earth and Planetary Science Letters 312, 91–101.

Janasi, V.A., Freitas, V.A., Heaman, L.H., 2011. The onset of flood basalt volcanism, Northern Paraná Basin, Brazil: a precise U–Pb baddeleyite/zircon age for a Chapecó-type dacite. Earth and Planetary Science Letters 302, 147–153.

Kawashita, K., 1972. O método Rb-Sr em rochas sedimentares. PhD thesis. Instituto de Geociências, IGc-USP, Brazil, p. 111.

Kelemen, P.B., Hanghøj, K., Greene, A.R., 2003. One view of the geochemistry of subduction-related magmatic arcs with an emphasis on primitive andesite and lower crust. In: Rudnick, R.L. (Ed.), Treatise on Geochemistry. The Earth's Crust, vol. 3. Elsevier, pp. 593–659.

King, S.D., Anderson, D.L., 1998. Edge-driven convection. Earth and Planetary Science Letters 160, 289–296.

Laux, J.H., Pimentel, M.M., Dantas, E.L., Armstrong, R., Junges, S.L., 2005. Two neoproterozoic crustal accretion events in the Brasília belt, central Brazil. Journal of South American Earth Sciences 18, 183–198.

Le Bas, M.J., Le Maitre, R.W., Streckeisen, A., Zannetin, B., 1986. A chemical classification of volcanic rocks based on total alkali-silica diagram. Journal of Petrology 27, 745–750.

Le Bas, M.J., Streckeisen, A.L., 1991. The IUGS systematics of igneous rocks. Journal of the Geological Society 148, 825–833.

Lustrino, M., 2005. How the delamination and detachment of lower crust can influence basaltic magmatismo. Earth Science Review 72, 21–38.

Marques, L.S., Dupré, B., Piccirillo, E.M., 1999. Mantle source compositions of the Paraná Magmatic Province: evidence from trace element and Sr–Nd–Pb isotope geochemistry. Journal of Geodynamics 28, 439–459.

McCullouch, M.T., Gamble, J.A., 1991. Geochemical and geodynamical constraints on subduction zone magmatism. Earth and Planetary Science Letters 102, 358–374.

Mcdonough, W.F., Sun, S.-S., 1995. The composition of the Earth. Chemical Geology 120, 223–253.

Meibom, A., Anderson, D.L., 2003. The statistical upper mantle assemblage. Earth and Planetary Science Letters 217, 123–139.

Nardy, A.J.R., Enzweiler, J., Bahia, F.O., Oliveira, M.A.F., Peneiro, M.A.V., 1997. Determinação de Elementos Maiores e Menores em Rochas Silicáticas por Espectometria de Fluorescência de Raios-X: Resultados Preliminares. In: Anais... Salvador. Congresso Brasileiro De Geoquímica, vol. 6, pp. 346–348. Salvador, BA.

Peate, D.W., Hawkesworth, C.J., Mantovani, M.S.M., 1992. Chemical stratigraphy of the Paraná lavas, South America: classification of magma types and their spatial distribution. Bulletin of Volcanology 55, 119–139.

Peate, D.W., Hawkesworth, C.J., Mantovani, M.S.M., Rogers, N.W., Turner, S.P., 1999. Petrogenesis and stratigraphy of the high-Ti/Y Urubici magma type in the Paraná flood basalt province and implications for the nature of 'Dupal'- type mantle in the South Atlantic region. Journal of Petrology 40 (3), 451–473.

Piccirillo, E.M., Melfi, A.J., 1988. The Mesozoic Flood Volcanism of the Paraná Basin: Petrogenetic and Geophysical Aspects. Universidade de São Paulo, São Paulo, p. 600.

Piccirillo, E.M., Bellieni, G., Cavazzini, G., Comin-Chiaramonti, P., Petrini, R., Melfi, A.J., Pinese, J.P.P., Zantadeschi, P., De Min, A., 1990. Lower Cretaceous tholeiitic dyke swarms from the Ponta Grossa Arch (southeast Brazil): petrology, Sr–Nd isotopes and genetic relationships with the Paraná flood volcanics. Chemical Geology 89, 19–48.

Pilet, S., Baker, M.B., Stolper, E.M., 2008. Metasomatized lithosphere and the origin of alkaline lavas. Science 320, 916–919.

Pimentel, M.M., Fuck, R.A., Gioia, S.M.C.L., 2000. The Neoproterozoic Goiás magmatic arc, central Brazil: a review and new Sm–Nd isotopic data. Revista Brasileira de Geociências 30 (1), 35–39.

Puchtel, I.S., Arndt, N.T., Hofmann, A.W., et al., 1998. Petrology of mafic lavas within the Onega plateau, central Karelia: evidence for 2.0 Ga plume-related continental crustal growth in the Baltic Shield. Contributions to Mineralogy and Petrology 130, 134–153.

Raposo, M.I.B., Ernesto, M., Renne, P.R., 1998. Paleomagnetic and $^{40}Ar/^{39}Ar$ data on the Early Cretaceous dike swarm from the Santa Catarina Island, Southern Brazil. Earth and Planetary Science Letters 108, 275–290.

Rehkämper, M., Hofmann, A.W., 1997. Recycled ocean crust and sediment in Indian Ocean MORB. Earth and Planetary Science Letters 147, 93–106.

Renne, P.R., Ernesto, M., Pacca, I.G., Coe, R.S., Glen, J., Prev, M., Perrin, M., 1992. The age of Parana flood volcanism, rifting of Gondwanaland, and the Jurassic – Cretaceous boundary. Science 258, 975–979.

Richardson, S.H., Erlank, A.J., Duncan, A.R., Reid, D.L., 1982. Correlated Nd, Sr, Pb isotope variation in Walvis Ridge basalts and implications for the evolution of their mantle source. Earth and Planetary Science Letters 59, 327–342.

Rocha-Júnior, E.R.V., 2011. Sistemática isotópica de Os–Nd–Pb–Sr e geoquímica de elementos traço litófilos e siderófilos de basaltos da Província Magmática do Paraná. Ph.D. Thesis. Universidade de São Paulo, Brazil, p. 153.

Rocha-Júnior, E.R.V., Puchtel, I.S., Marques, L.S., Walker, R.J., Machado, F.B., Nardy, A.J.R., Babinski, M., Figueiredo, A.M.G., 2012. Re–Os isotope and highly siderophile element systematics of the Paraná Continental Flood Basalts (Brazil). Earth and Planetary Science Letters 337–338, 164–173.

Salters, V.J.M., Sachi-Kocher, A., 2010. An ancient metasomatic source for the Walvis Ridge basalts. Chemical Geology 273, 151–167.

Sato, K., Tassinari, C.G.C., Kawashita, K., Petronillo, L., 1995. O método geocronológico Sm-Nd no IG-USP e suas aplicações. Anais da Academia Brasileira de Ciências 67, 313–336.

Sheth, H.C., 2005. Were the Deccan flood basalts derived impart from ancient oceanic crust within the Indian continental lithosphere? Gondwana Research 8, 109–127.

Shirey, S.B., Walker, R.J., 1998. The Re–Os isotope system in cosmochemistry and high-temperature geochemistry. Annual Review of Earth and Planetary Sciences 26, 423–500.

Sobolev, A.V., Hofmann, A.W., Sobolev, S.V., Nikogosian, I.K., 2005. An olivine-free mantle source of Hawaiian shield basalts. Nature 434, 590–597.

Sobolev, A.V., , et al.(19 outros autores), 2007. The amount of recycled crust in sources of mantle-derived melts. Science 316, 412–417.

Sun, S.-S., McDonough, W.F., 1989. Chemical and isotope systematics of oceanic basalts: implications for mantle composition and processes. In: Saunders, A.D., Norry, M.J. (Eds.), Magmatism in the Ocean Basins. Geological Society, London, pp. 313–345.

Tatsumoto, M., Basu, A.R., Wankang, H., Junwen, W., Guanghong, X., 1992. Sr, Nd, and Pb isotopes of ultramafic xenoliths in volcanic rocks of Eastern China: enriched components EMI and EMII in subcontinental lithosphere. Earth and Planetary Sciences Letters 113, 107–128.

Thiede, D.S., Vasconcelos, P.M., 2010. Paraná flood basalts: rapid extrusion hypothesis confirmed by new $^{40}Ar/^{39}Ar$ results. Geology 38 (8), 747–750.

Thompson, R.N., Gibson, S.A., Mitchell, J.G., Dickin, A.P., Leonardos, O.H., Brod, J.A., Greenwood, J.C., 1998. Migrating Cretaceous-Eocene magmatism in the Serra do Mar alkaline province, SE Brazil: melts from the deflected Trindade mantle plume? Journal of Petrology 39 (8), 1493–1526.

Tohver, E., Trindade, R.I.F., Solum, J.G., Hall, C.M., Riccomini, C., Nogueira, A.C., 2010. Closing the Clymene ocean and bending a Brasiliano belt: evidence for the Cambrian formation of Gondwana, southeast Amazon craton. Geology 38, 267–270.

Toyoda, K., Horiuchi, H., Tokonami, M., 1994. Dupal anomaly of the Brazilian carbonatites: geochemical correlations with hotspots in the South Atlantic and implications for the mantle source. Earth and Planetary Science Letters 126, 315–331.

Turner, S., Regelous, M., Kelley, S., Hawkesworth, C.J., Mantovani, M., 1994. Magmatism and continental break-up in the South Atlantic: high precision $^{40}Ar–^{39}Ar$ geochronology. Earth and Planetary Science Letters 121, 333–348.

Valeriano, C.M., Pimentel, M.M., Heilbron, M., Almeida, J.C.H., Trouw, R.A.J., 2008. Tectonic evolution of the Brasília Belt, Central Brazil, and early assembly of Gondwana. In: Pankhurst, R.J., et al. (Eds.), 2008. West Gondwana: Pre-cenozoic Correlations across the South Atlantic Region, vol. 294. Geological Society, London, pp. 197–210. Special Publications.

Walker, R.J., Prichard, H.M., Ishiwatari, A., Pimentel, M.M., 2002. The osmium isotopic composition of convecting upper mantle deduced from ophiolite chromitites. Geochimica et Cosmochimica Acta 66, 329–345.
Weaver, B.L., 1991. The origin of ocean island basalt end-member compositions: trace element and isotopic constraints. Earth and Planetary Science Letters 104, 381–397.
White, R., McKenzie, D.J., 1989. Magmatism at rift zones: the generation of volcanic continental margins and flood basalts. Journal of Geophysical Research 94 (B6), 7685–7729.
Widom, E., 2011. Recognizing recycled osmium. Geology 39 (11), 1087–1088.
Yaxley, G.M., Green, D.H., 1998. Reactions between eclogite and peridotite: mantle refertilization by subducted oceanic crust. Schweizerische Mineralogische und Petrographische Mitteilungen 78, 243–255.
Yaxley, G.M., 2000. Experimental study of the phase and melting relations of homogeneous basalt + peridotite mixtures and implications for the petrogenesis of food basalts. Contributions to Mineralogy and Petrology 139, 326–338.
Zindler, A., Hart, S.R., 1986. Chemical geodynamics. Annual Reviews of Earth and Planetary Sciences 14, 493–571.